D-Instanton Effects on The Holographic Weyl Semimetals

Yunseok Seo(Kookmin Univ.)

July 23, 2026

arXiv:2604.04424 with Hwajin Eom(Ajou U.)

Introduction

- Weyl semimetal
  - Semimetals whose quasiparticle excitation is the Weyl fermion
  - Band inversion at two Weyl point
  - Broken parity or time-reversal symmetry: Dirac ferminon → left-, right-handed Weyl fermion
  - TaAs, TaP, NbAs, NbP(P-broken), magnetic WSMs $Co_3Sn_2S_2$, Co_2MnGa(T-broken) and AHE

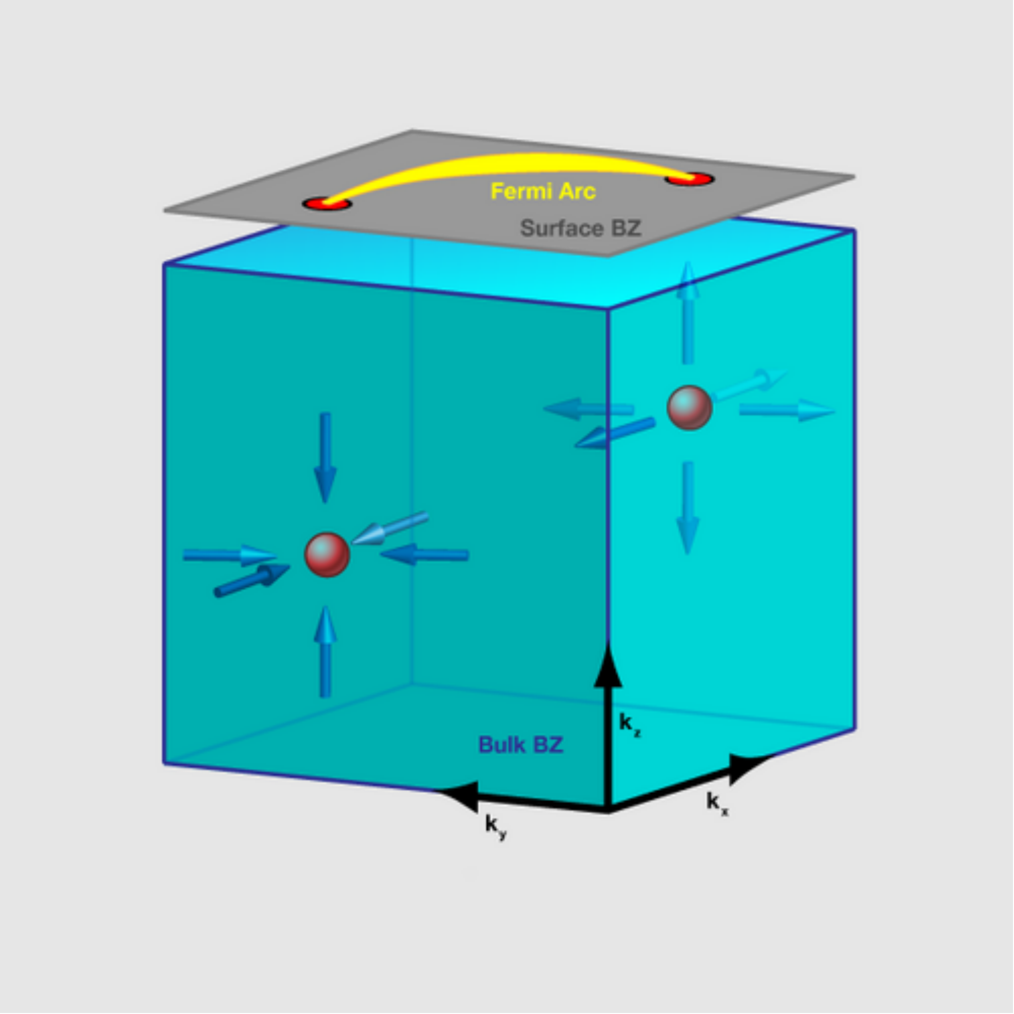

Introduction

- Weyl semimetal
  - Free Dirac fermion with non-dynamical axial vector field

$$\mathcal{L} = \bar{\psi}\left(i\gamma^\mu\partial_\mu - m + \underline{A_j^5\gamma^j\gamma^5}\right)\psi,$$

Breaks time-reversal symmetry

Introduction

- Weyl semimetal
  - Free Dirac fermion with non-dynamical axial vector field

$$\mathcal{L} = \bar{\psi}\left(i\gamma^\mu\partial_\mu - m + \underline{A_j^5\gamma^j\gamma^5}\right)\psi,$$

Breaks time-reversal symmetry

  - Set $A_j^5 = \frac{b}{2}\delta_{jz}$

$$\varepsilon = \pm\sqrt{k_x^2 + k_y^2 + \left(\frac{b}{2} \pm \sqrt{k_z^2 + m^2}\right)^2}$$

- $\left|\frac{m}{b}\right| < \frac{1}{2}$: $\varepsilon = 0$ at $(k_x, k_y, ,k_z) = \left(0,\ 0,\ \pm\sqrt{(b/2)^2 - m^2}\right)$, WSM
- $\left|\frac{m}{b}\right| > \frac{1}{2}$: $\varepsilon > 0$, Trivial insulator
- $\left|\frac{m}{b}\right| = \frac{1}{2}$: $\varepsilon = 0$ at $(k_x, k_y, ,k_z) = (0,\ 0,\ 0)$, Dirac fermion

Introduction

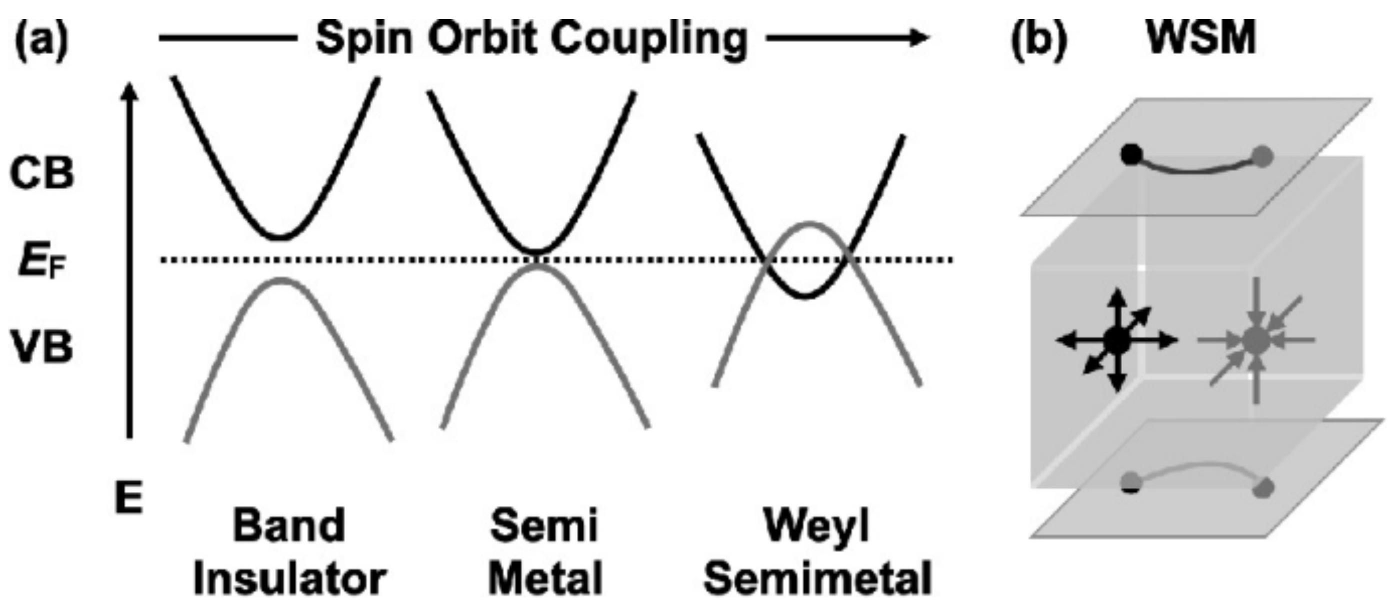

- Set $A_j^5 = \frac{b}{2}\delta_{jz}$

$$\varepsilon = \pm\sqrt{k_x^2 + k_y^2 + \left(\frac{b}{2} \pm \sqrt{k_z^2 + m^2}\right)^2}$$

- $\left|\frac{m}{b}\right| < \frac{1}{2}$: $\varepsilon = 0$ at $(k_x, k_y, , k_z) = \left(0,\ 0,\ \pm\sqrt{(b/2)^2 - m^2}\right)$, WSM
- $\left|\frac{m}{b}\right| > \frac{1}{2}$: $\varepsilon > 0$, Trivial insulator
- $\left|\frac{m}{b}\right| = \frac{1}{2}$: $\varepsilon = 0$ at $(k_x, k_y, , k_z) = (0, 0, 0)$, Dirac fermion

Introduction

■ Strong interaction in Dirac materials?

o Violation of Wiedeman-Frantz law in graphene

ELECTRON TRANSPORT

Observation of the Dirac fluid and the breakdown of the Wiedemann-Franz law in graphene

Jesse Crossno,[1,2] Jing K. Shi,[1] Ke Wang,[1] Xiaomeng Liu,[1] Achim Harzheim,[1] Andrew Lucas,[1] Subir Sachdev,[1,3] Philip Kim,[1,2*] Takashi Taniguchi,[4] Kenji Watanabe,[4] Thomas A. Ohki,[5] Kin Chung Fong[5*]

Interactions between particles in quantum many-body systems can lead to collective behavior described by hydrodynamics. One such system is the electron-hole plasma in graphene near the charge-neutrality point, which can form a strongly coupled Dirac fluid. This charge-neutral plasma of quasi-relativistic fermions is expected to exhibit a substantial enhancement of the thermal conductivity, thanks to decoupling of charge and heat currents within hydrodynamics. Employing high-sensitivity Johnson noise thermometry, we report an order of magnitude increase in the thermal conductivity and the breakdown of the Wiedemann-Franz law in the thermally populated charge-neutral plasma in graphene. This result is a signature of the Dirac fluid and constitutes direct evidence of collective motion in a quantum electronic fluid.

(Science, 2016)

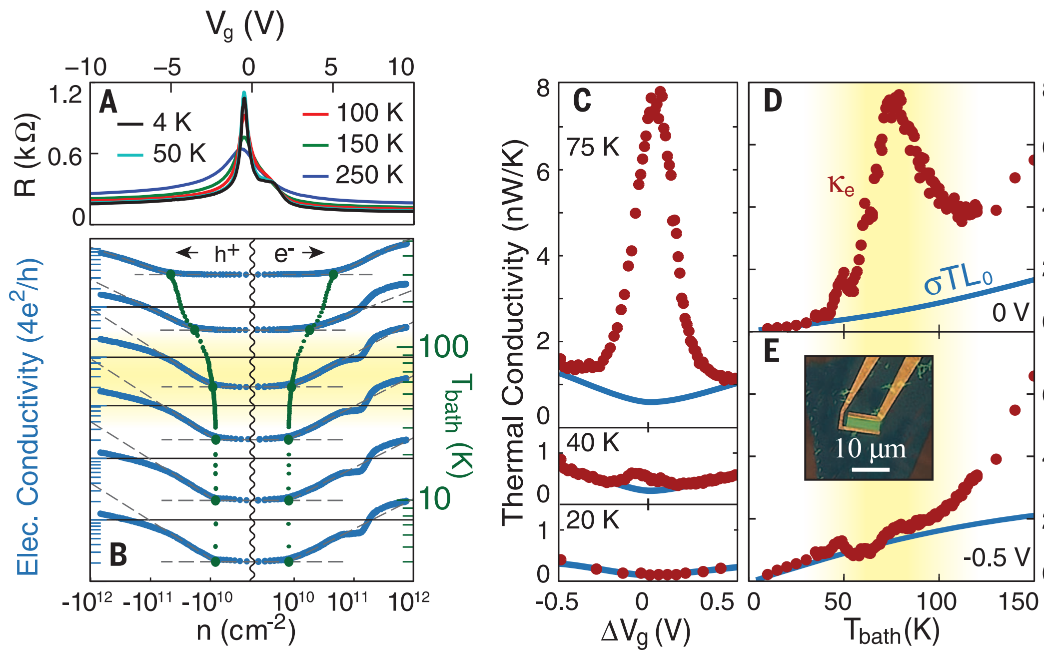

o Surface state of topological insulator

SCIENTIFIC REPORTS

OPEN

Quantum Corrections Crossover and Ferromagnetism in Magnetic Topological Insulators

SUBJECT AREAS:
MATERIALS FOR DEVICES
ELECTRICAL AND ELECTRONIC ENGINEERING
ELECTRONIC DEVICES
MAGNETIC PROPERTIES AND MATERIALS

Received 24 April 2013
Accepted 15 July 2013
Published 9 August 2013

Correspondence and requests for materials

Lihong Bao[1,2*], Weiyi Wang[1*], Nicholas Meyer[2*], Yanwen Liu[1], Cheng Zhang[1], Kai Wang[1,2], Ping Ai[1] & Faxian Xiu[1]

[1]State Key Laboratory of Surface Physics and Department of Physics, Fudan University, Shanghai 200433, China, [2]Department of Electrical and Computer Engineering, Iowa State University, Ames, IA 50010, USA.

Revelation of emerging exotic states of topological insulators (TIs) for future quantum computing applications relies on breaking time-reversal symmetry and opening a surface energy gap. Here, we report on the transport response of Bi_2Te_3 TI thin films in the presence of varying Cr dopants. By tracking the magnetoconductance (MC) in a low doping regime we observed a progressive crossover from weak antilocalization (WAL) to weak localization (WL) as the Cr concentration increases. In a high doping regime, however, increasing Cr concentration yields a monotonically enhanced anomalous Hall effect (AHE) accompanied by an increasing carrier density. Our results demonstrate a possibility of manipulating bulk ferromagnetism and quantum transport in magnetic TI, thus providing an alternative way for experimentally realizing exotic quantum states required by spintronic applications.

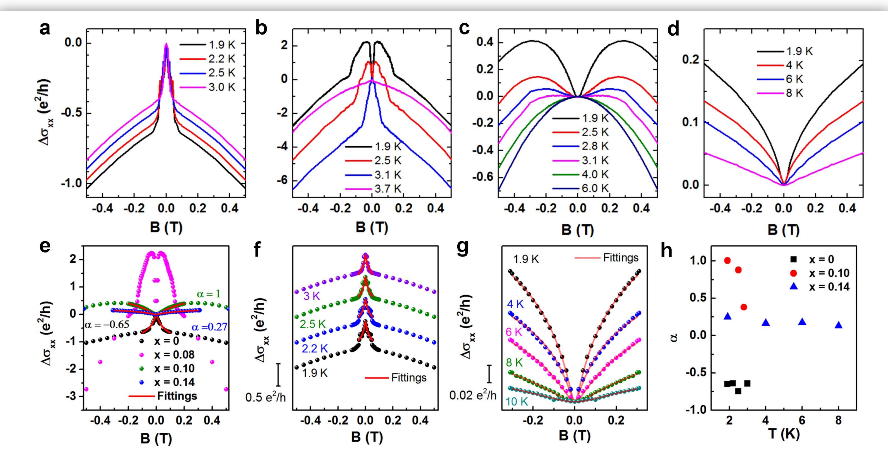

Figure 2 | Crossover of quantum corrections of magnetoconductance (MC) with increasing Cr content in $Cr_xBi_{2-x}Te_3$ thin films ($x \leq 0.14$). (a) MC curves of pure Bi_2Te_3 thin films, showing the negative MC features of WAL. (b) MC curves of $Cr_{0.08}Bi_{1.92}Te_3$ thin film, indicating a non-monotonic behavior with sharp downward cusp at low temperatures (< 3.1 K) and re-presence of WAL at higher temperatures (3.1 and 3.7 K). (c) MC curves of $Cr_{0.10}Bi_{1.90}Te_3$ thin film, showing a crossover from downward cusp feature to parabolic dependence with increasing temperatures. (d) MC curves of $Cr_{0.14}Bi_{1.86}Te_3$ thin film shows a WL dominated behavior. (e) HLN model fitting of MC curves with different Cr content at temperature of 1.9 K. (f) and (g) HLN model fitting of MC curves of pure Bi_2Te_3 and heavily doped $Cr_{0.14}Bi_{1.86}Te_3$ thin films, showing that both WAL and WL can be fitted well to the HLN model. (h) Pre-factor of α in HLN model of thin films with different Cr concentrations.

Introduction

- Strong interaction in Dirac materials?
  - Fermi energy is near the Dirac point → small Fermi surface → reduced screening → strong interaction
  - Gauge/gravity duality
    - Strongly interacting D-dimensional gauge theory can correspond to the classical gravity in D+1 dimension
    - AdS/CFT correspondence: $4D\ \mathcal{N}=4,\ SYM \leftrightarrow AdS_5 \times S^5$
    - Strong interaction in QCD: $\frac{\eta}{s} \sim \frac{1}{4\pi}$ in quark-gluon plasma in RHIC
    - Extended to strongly interacting condensed matter system: Holographic superconductor

Introduction

■ Strong interaction in Dirac materials?

○ Violation of Wiedeman-Frantz law in graphene

Holography of the Dirac Fluid in Graphene with two currents #18

Yunseok Seo (Hanyang U.), Geunho Song (Hanyang U.), Philip Kim (Harvard U., Phys. Dept. and Seoul Natl. U.), Subir Sachdev (Harvard U., Phys. Dept. and Perimeter Inst. Theor. Phys.), Sang-Jin Sin (Hanyang U.) (Sep 12, 2016)

Published in: *Phys.Rev.Lett.* 118 (2017) 3, 036601 • e-Print: 1609.03582 [hep-th]

pdf DOI cite claim reference search 54 citations

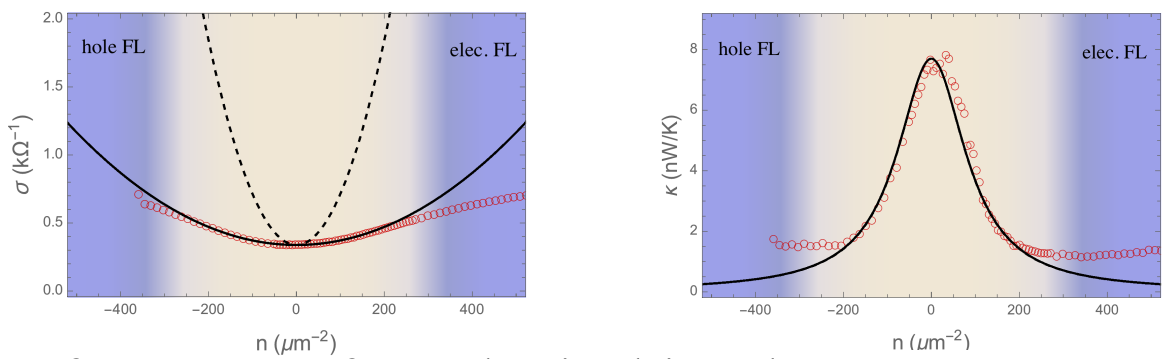

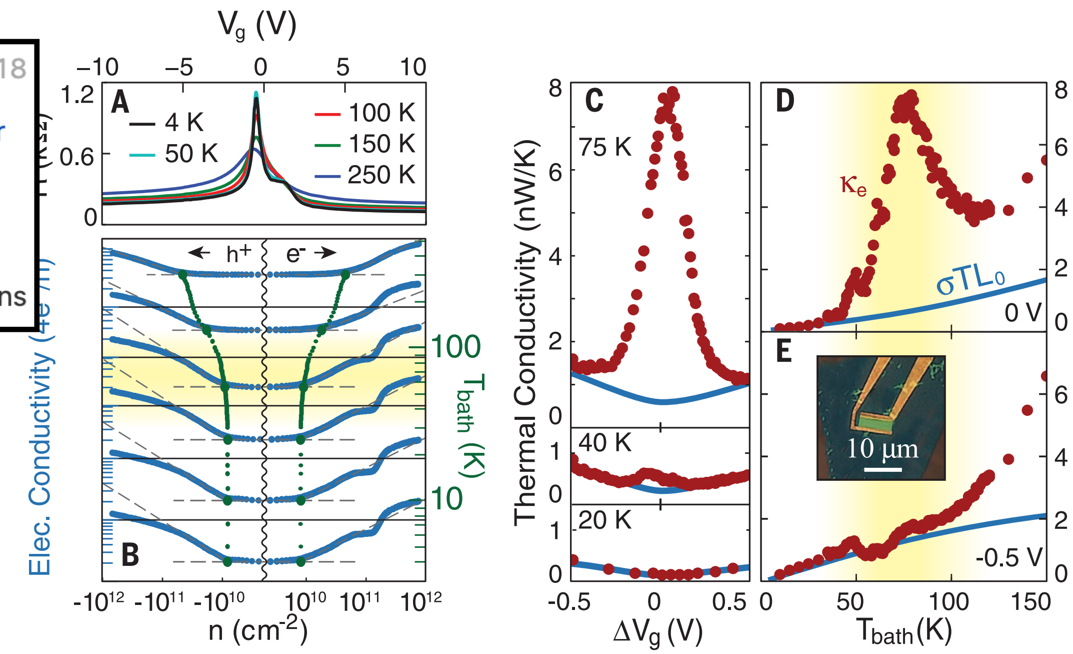

○ Surface state of topological insulator

Strong Correlation Effects on Surfaces of Topological Insulators via Holography #17

Yunseok Seo (Hanyang U.), Geunho Song (Hanyang U.), Sang-Jin Sin (Hanyang U.) (Mar 21, 2017)

Published in: *Phys.Rev.B* 96 (2017) 4, 041104 • e-Print: 1703.07361 [hep-th]

pdf DOI cite claim reference search 19 citations

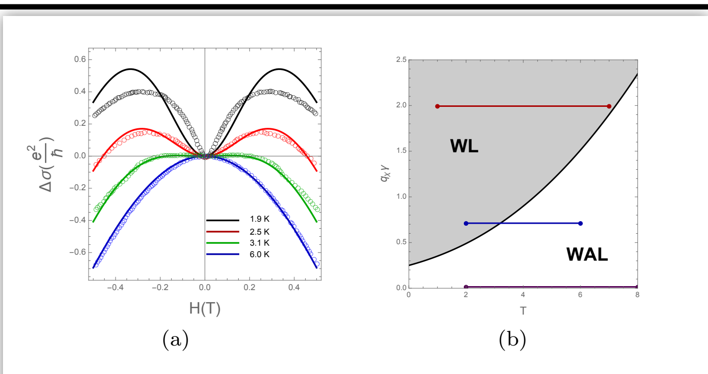

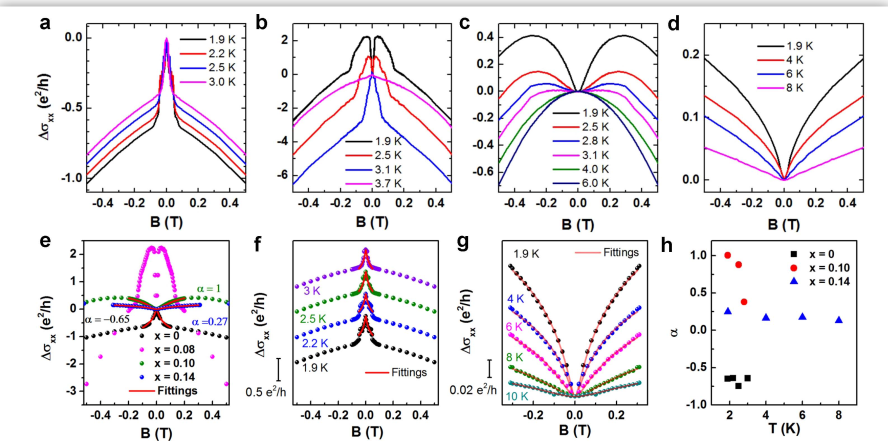

Figure 2 | Crossover of quantum corrections of magnetoconductance (MC) with increasing Cr content in $Cr_xBi_{2-x}Te_3$ thin films ($x \leq 0.14$). (a) MC curves of pure Bi_2Te_3 thin films, showing the negative MC features of WAL. (b) MC curves of $Cr_{0.08}Bi_{1.92}Te_3$ thin film, indicating a non-monotonic behavior with sharp downward cusp at low temperatures (< 3.1 K) and re-presence of WAL at higher temperatures (3.1 and 3.7 K). (c) MC curves of $Cr_{0.10}Bi_{1.90}Te_3$ thin film, showing a crossover from downward cusp feature to parabolic dependence with increasing temperatures. (d) MC curves of $Cr_{0.14}Bi_{1.86}Te_3$ thin film shows a WL dominated behavior. (e) HLN model fitting of MC curves with different Cr content at temperature of 1.9 K. (f) and (g) HLN model fitting of MC curves of pure Bi_2Te_3 and heavily doped $Cr_{0.14}Bi_{1.86}Te_3$ thin films, showing that both WAL and WL can be fitted well to the HLN model. (h) Pre-factor of α in HLN model of thin films with different Cr concentrations.

Holograhpic Weyl Semimetal

- Holograpy for Weyl semimetal
  - Semi-holography: Mix of non-holographic fermion with holgorphic CFT(AdS)
    - Non-integer scaling of the conductivity in frequency and temperature

U. Gürsoy, V. Jacobs, E. Plauschinn, H. Stoof and S. Vandoren, *Holographic models for undoped Weyl semimetals*, *JHEP* **04** (2013) 127 [arXiv:1209.2593] [INSPIRE].

V.P.J. Jacobs, P. Betzios, U. Gürsoy and H.T.C. Stoof, *Electromagnetic response of interacting Weyl semimetals*, *Phys. Rev. B* **93** (2016) 195104 [arXiv:1512.04883] [INSPIRE].

T. Faulkner and J. Polchinski, *Semi-Holographic Fermi Liquids*, *JHEP* **06** (2011) 012 [arXiv:1001.5049] [INSPIRE].

U. Gürsoy, E. Plauschinn, H. Stoof and S. Vandoren, *Holography and ARPES Sum-Rules*, *JHEP* **05** (2012) 018 [arXiv:1112.5074] [INSPIRE].

Holograhpic Weyl Semimetal

- Holograpy for Weyl semimetal
  - Bottom-up approach: Einstein-Hibert gravity + complex scalar + two U(1) + CS term
    - Quantum transition between WSM and trivial semimeta via Lifshitz critical point
    - Various studies for Fermi arcs, odd viscosity, chaos, etc.

K. Landsteiner and Y. Liu, *The holographic Weyl semi-metal*, *Phys. Lett. B* **753** (2016) 453 [arXiv:1505.04772] [INSPIRE].

K. Landsteiner, Y. Liu and Y.-W. Sun, *Quantum phase transition between a topological and a trivial semimetal from holography*, *Phys. Rev. Lett.* **116** (2016) 081602 [arXiv:1511.05505] [INSPIRE].

C. Copetti, J. Fernández-Pendás and K. Landsteiner, *Axial Hall effect and universality of holographic Weyl semi-metals*, *JHEP* **02** (2017) 138 [arXiv:1611.08125] [INSPIRE].

Y. Liu and J. Zhao, *Weyl semimetal/insulator transition from holography*, *JHEP* **12** (2018) 124 [arXiv:1809.08601] [INSPIRE].

K. Landsteiner, Y. Liu and Y.-W. Sun, *Holographic topological semimetals*, *Sci. China Phys. Mech. Astron.* **63** (2020) 250001 [arXiv:1911.07978] [INSPIRE].

Holograhpic Weyl Semimetal

- Holograpy for Weyl semimetal
  - Top-down approach: D3-D7 system

A Weyl semimetal from AdS/CFT with flavour #2

Kazem Bitaghsir Fadafan (Shahrood U.), Andy O'Bannon (Southampton U.), Ronnie Rodgers (Utrecht U. (main)), Matthew Russell (Southampton U.) (Dec 21, 2020)

Published in: *JHEP* 04 (2021) 162 • e-Print: 2012.11434 [hep-th]

pdf DOI cite claim reference search 23 citations

Holograhpic Weyl Semimetal

- Holograpy for Weyl semimetal
  - Top-down approach: D3-D7 system

A Weyl semimetal from AdS/CFT with flavour #2

Kazem Bitaghsir Fadafan (Shahrood U.), Andy O'Bannon (Southampton U.), Ronnie Rodgers (Utrecht U. (main)), Matthew Russell (Southampton U.) (Dec 21, 2020)

Published in: *JHEP* 04 (2021) 162 • e-Print: 2012.11434 [hep-th]

pdf DOI cite claim reference search 23 citations

		x_0	x_1	x_2	x_3	x_4	x_5	x_6	x_7	x_8	x_9
N_C	D3	×	×	×	×						
N_F	D7	×	×	×	×	×	×	×	×		

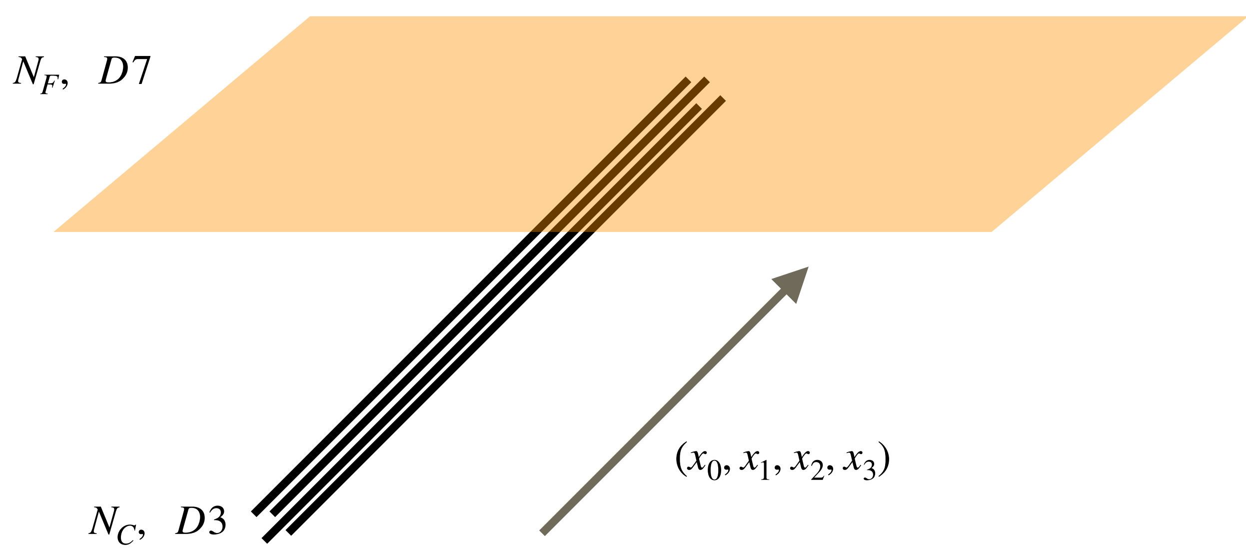

Holograhpic Weyl Semimetal

■ Holograpy for Weyl semimetal

		x_0	x_1	x_2	x_3	x_4	x_5	x_6	x_7	x_8	x_9
N_C	D3	×	×	×	×						
N_F	D7	×	×	×	×	×	×	×	×		

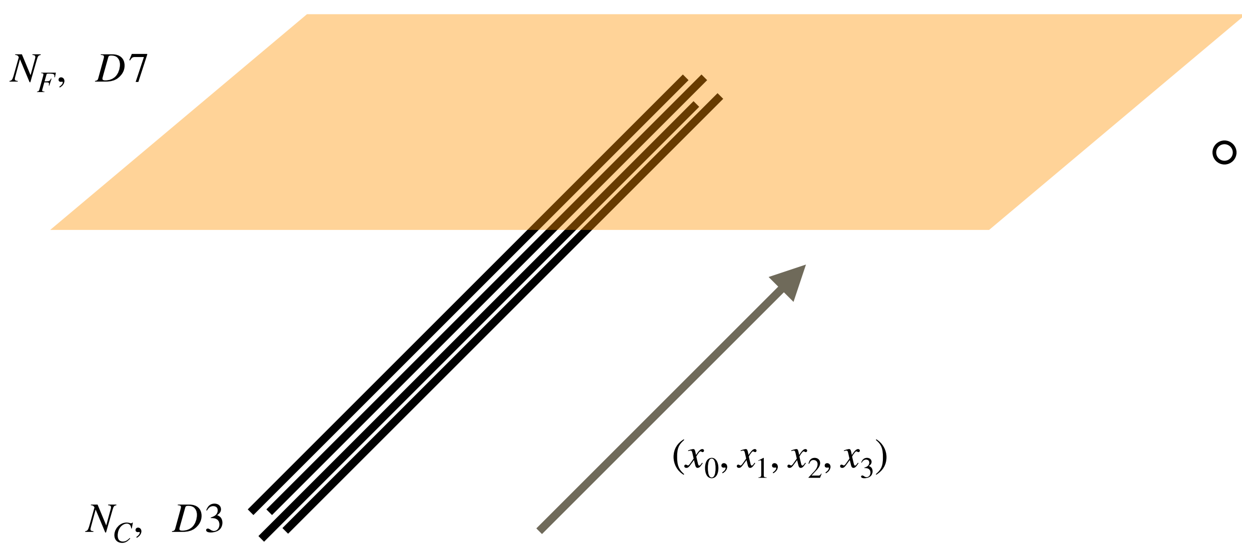

$$W(x,r) = x_8 + i x_9 = \rho(r) e^{i\phi(x)}$$

- Fermion fluctuations

$$S \sim \int d^8\xi \sqrt{-g}\,\bar{\Psi}\left(\gamma^\mu D_\mu + \cdots\right)\Psi$$

$$\bar{\Psi}\left(\frac{i}{2}\gamma^\mu \partial_\mu \phi \Gamma^{89}\right)\Psi$$

Γ^{89} generates rotations in the (x_8, x_9) plane.

Holograhpic Weyl Semimetal

■ Holograpy for Weyl semimetal

		x_0	x_1	x_2	x_3	x_4	x_5	x_6	x_7	x_8	x_9
N_C	D3	×	×	×	×						
N_F	D7	×	×	×	×	×	×	×	×		

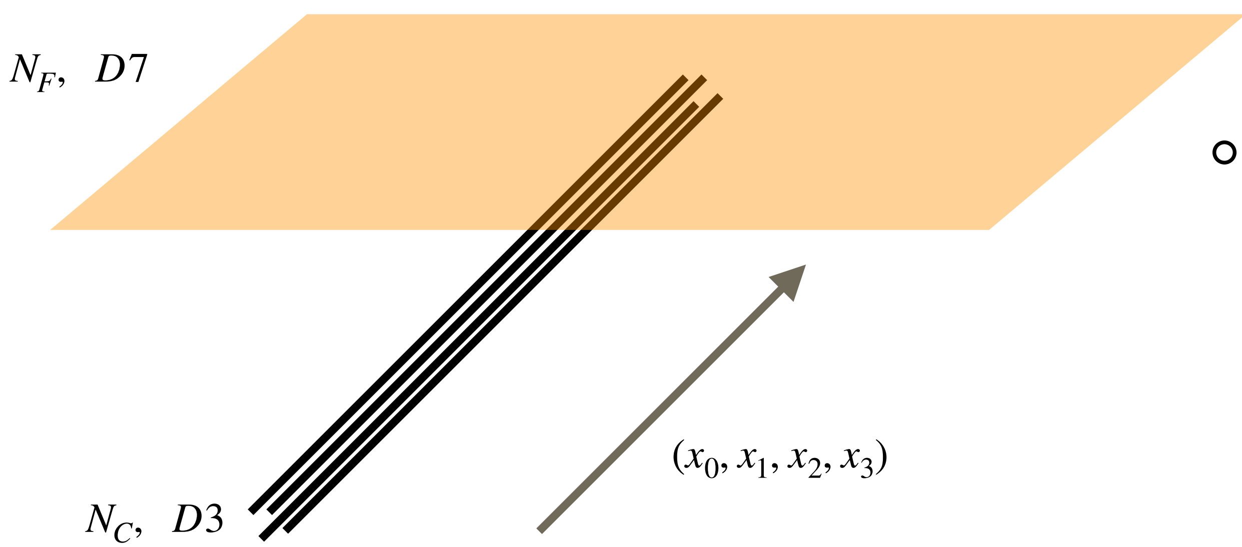

$$W(x,r) = x_8 + i x_9 = \rho(r) e^{i\phi(x)}$$

∘ Fermion fluctuations

$$S \sim \int d^8\xi \sqrt{-g}\,\bar{\Psi}\left(\gamma^\mu D_\mu + \cdots\right)\Psi$$

$$\bar{\Psi}\left(\frac{i}{2}\gamma^\mu \partial_\mu \phi \Gamma^{89}\right)\Psi$$

Γ^{89} generates rotations in the (x_8, x_9) plane.

$$\Gamma^{89} \longrightarrow \pm\gamma_5.$$

$$\bar{\psi}\gamma^\mu(\partial_\mu\phi)\gamma_5\psi.$$

Holograhpic Weyl Semimetal

■ Holograpy for Weyl semimetal

		x_0	x_1	x_2	x_3	x_4	x_5	x_6	x_7	x_8	x_9
N_C	D3	×	×	×	×						
N_F	D7	×	×	×	×	×	×	×	×		

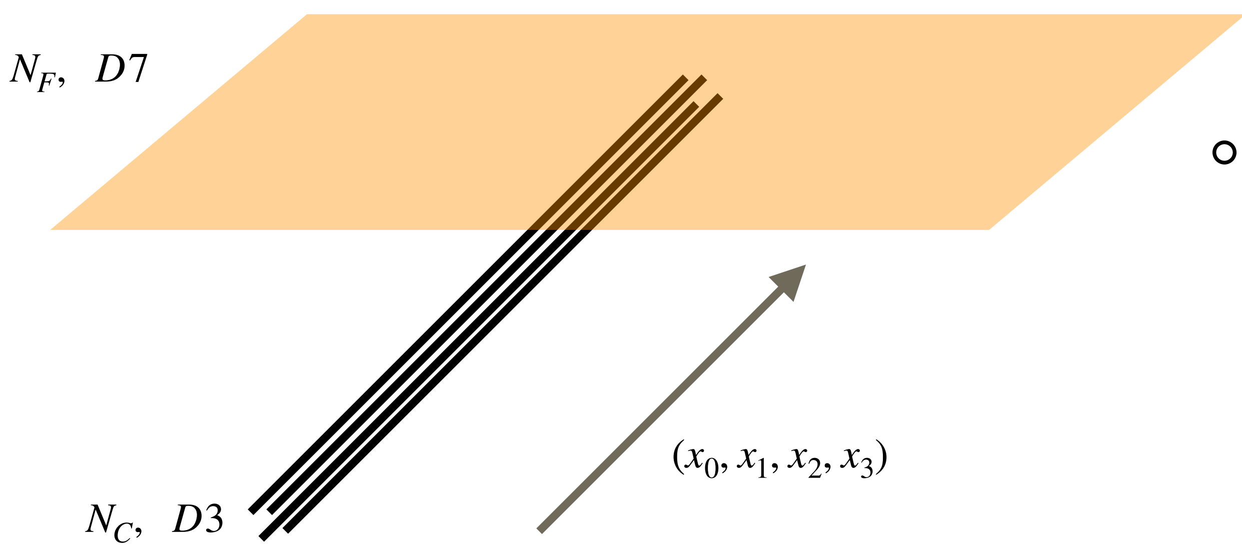

$$W(x,r) = x_8 + i x_9 = \rho(r) e^{i\phi(x)}$$

- Fermion fluctuations

$$S \sim \int d^8\xi \sqrt{-g}\,\bar{\Psi}\left(\gamma^\mu D_\mu + \cdots\right)\Psi$$

$$\bar{\Psi}\left(\frac{i}{2}\gamma^\mu \partial_\mu \phi \Gamma^{89}\right)\Psi$$

$$\mathcal{L}_\psi = i\bar{\psi}\left(i\gamma^\mu\partial_\mu - m + \frac{\partial_\mu\phi}{2}\gamma^\mu\gamma^5\right)\psi,$$

Holograhpic Weyl Semimetal

■ Holograpy for Weyl semimetal

		x_0	x_1	x_2	x_3	x_4	x_5	x_6	x_7	x_8	x_9
N_C	D3	×	×	×	×						
N_F	D7	×	×	×	×	×	×	×	×		

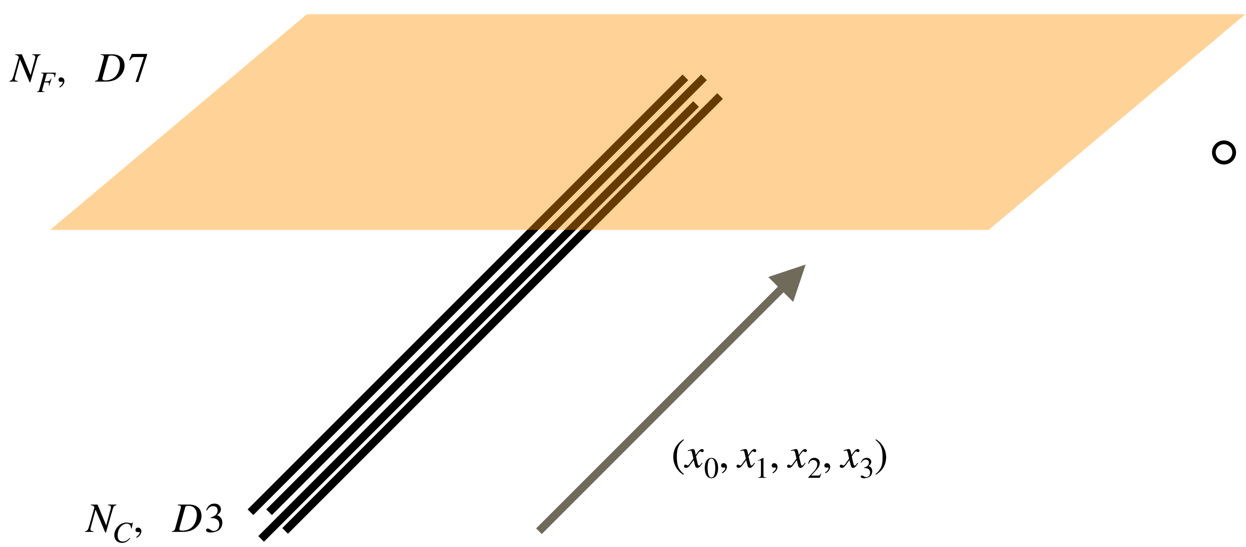

$$W(x, r) = x_8 + i x_9 = \rho(r) e^{i\phi(x)}$$

∘ Fermion fluctuations

$$S \sim \int d^8\xi \sqrt{-g}\,\bar{\Psi}\left(\gamma^\mu D_\mu + \cdots\right)\Psi$$

$$\bar{\Psi}\left(\frac{i}{2}\gamma^\mu \partial_\mu \phi \Gamma^{89}\right)\Psi$$

$$\mathcal{L}_\psi = i\bar{\psi}\left(i\gamma^\mu\partial_\mu - m + \frac{\partial_\mu\phi}{2}\gamma^\mu\gamma^5\right)\psi, \qquad \mathcal{L} = \bar{\psi}\left(i\gamma^\mu\partial_\mu - m + A^5_j\gamma^j\gamma^5\right)\psi, \quad A^5_j = \frac{b}{2}\delta_{jz}$$

$$A^5_\mu = \frac{\partial_\mu \phi}{2} \quad \text{with} \quad \phi = bz$$

Holograhpic Weyl Semimetal

■ Holograpy for Weyl semimetal

- D7 brane embeddings

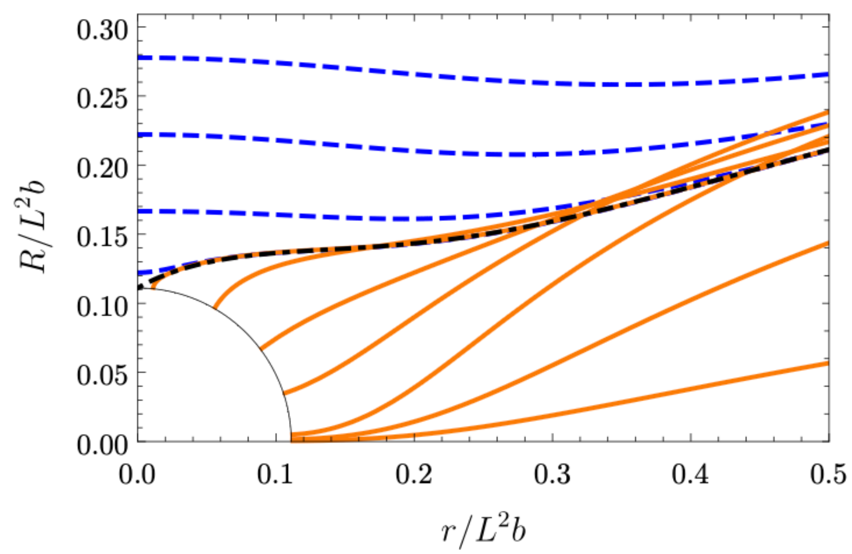

(a) Embeddings at $T/b = 0.05$.

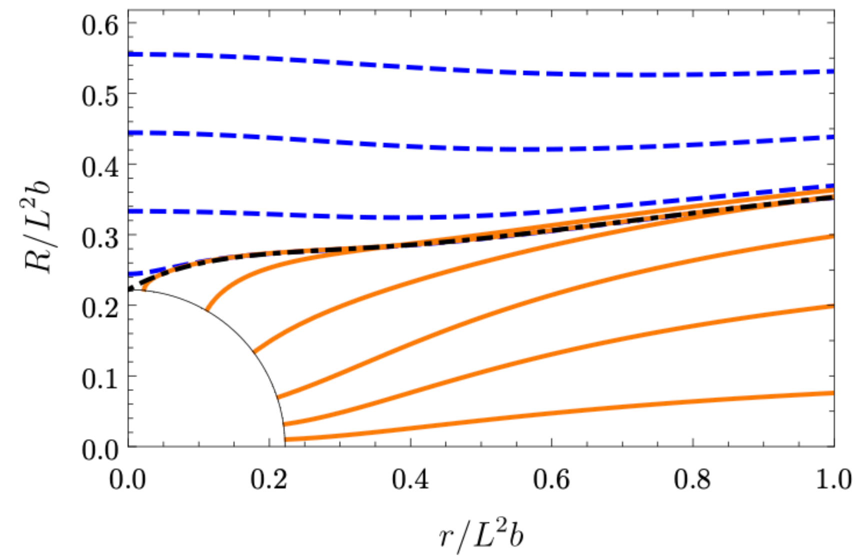

(b) Embeddings at $T/b = 0.1$.

- Phase diagram

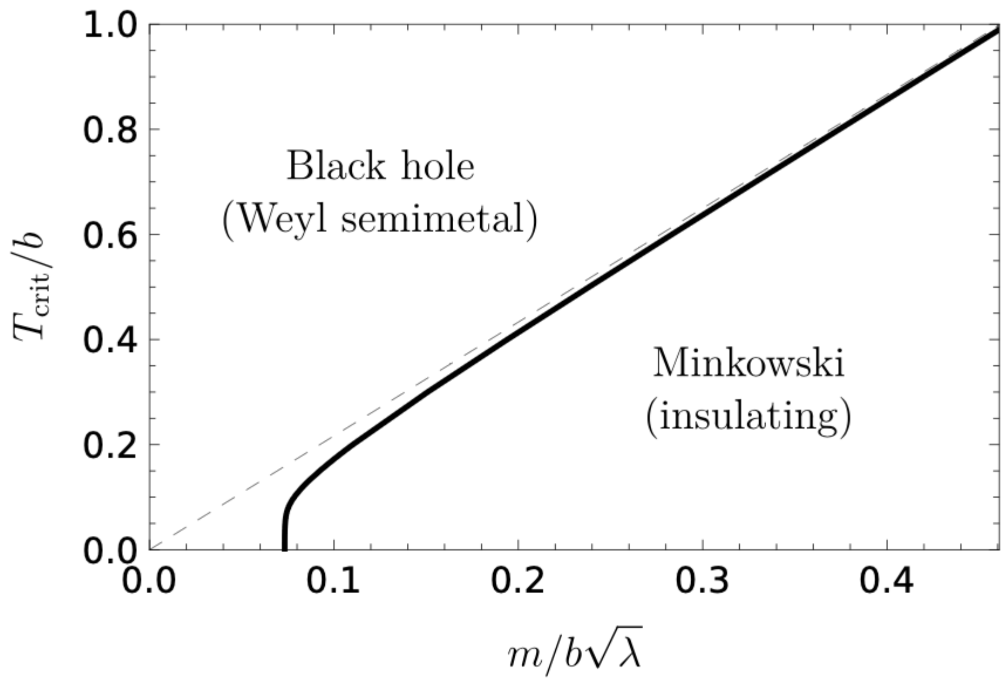

Holograhpic Weyl Semimetal

■ Holograpy for Weyl semimetal

Conductivities and excitations of a holographic flavour brane Weyl semimetal #1

Haruki Furukawa (Illinois U., Chicago), Sacha Ployet (U. Paris-Saclay), Ronnie Rodgers (Nordita and Royal Inst. Tech., Sodertalje) (Dec 20, 2024)

Published in: *JHEP* 07 (2025) 115 • e-Print: 2412.15827 [hep-th]

pdf DOI cite claim reference search 1 citation

Lifshitz transition in a holographic finite density flavor brane Weyl semimetal #2

Cheng-Yuan Lu (Shanghai U.), Xian-Hui Ge (Shanghai U. and SKLHTS, Shanghai), Sang-Jin Sin (Hanyang U.) (Sep 29, 2025)

Published in: *Phys.Rev.D* 113 (2026) 2, 026028 • e-Print: 2509.24287 [hep-th]

pdf DOI cite claim reference search 1 citation

Motivation

■ Can we add some impurities which can change the electronic property of WSM?

Holographic D Instanton Liquid and chiral transition #27

Bogeun Gwak (Sogang U. and CQUeST, Seoul), Minkyoo Kim (Sogang U. and CQUeST, Seoul), Bum-Hoon Lee (Sogang U. and CQUeST, Seoul), Yunseok Seo (CQUeST, Seoul), Sang-Jin Sin (Hanyang U.) (Mar, 2012)

Published in: *Phys.Rev.D* 86 (2012) 026010 • e-Print: 1203.4883 [hep-th]

pdf DOI cite claim reference search 30 citations

- D3-D(-1)-D7 system

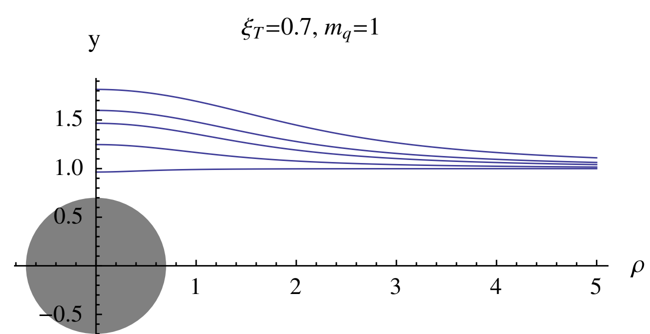

(a)

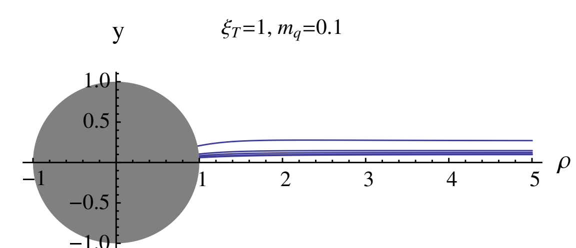

(b)

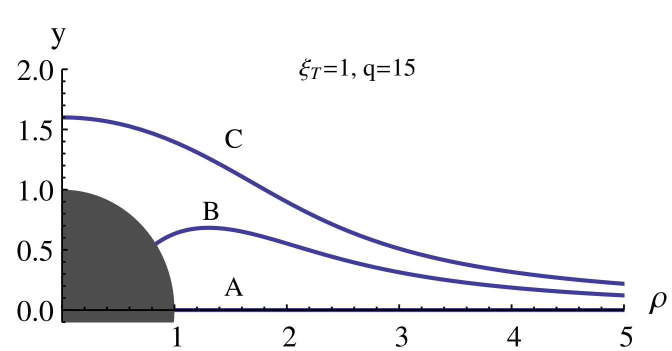

(b)

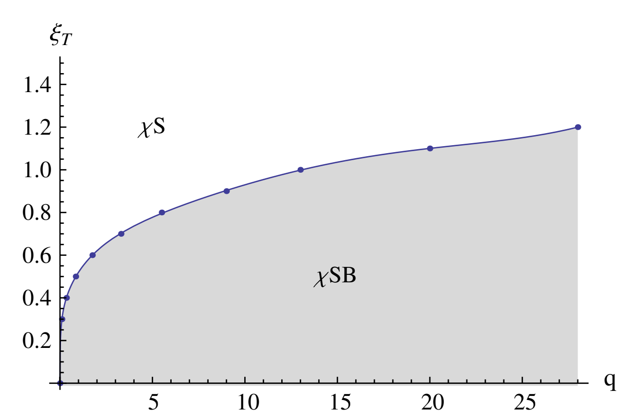

Holographic WSM with D-instantons

- Background geoemtry
  - SUGRA action for D3-D(-1) system

$$S = \frac{1}{\kappa}\int d^{10}x\sqrt{-g}\left(R - \frac{1}{2}\left(\partial\Phi\right)^2 + \frac{1}{2}e^{2\Phi}\left(\partial\chi\right)^2 - \frac{1}{6}F_{(5)}^2\right)$$

  - Background solution(in string frame)

$$ds_{10}^2 = e^{\Phi/2}\left[\frac{r^2}{L^2}\left(-f(r)^2dt^2 + d\vec{x}^2\right) + \frac{1}{f(r)^2}\frac{L^2}{r^2}dr^2 + L^2d\Omega_5^2\right],$$

$$e^{\Phi} = 1 + \frac{q}{r_H^4}\log\frac{1}{f(r)^2}, \quad \chi = -e^{-\Phi} + \chi_0, \quad f(r) = \sqrt{1 - \left(\frac{r_H}{r}\right)^4},$$

  - Dimensionless coordinates $\frac{d\xi^2}{\xi^2} = \frac{dr^2}{r^2 f(r)^2}$

$$ds_{10}^2 = e^{\Phi/2}\left[\frac{r^2}{L^2}\left(-f(r)^2dt^2 + d\vec{x}^2\right) + \frac{L^2}{\xi^2}\left(d\xi^2 + \xi^2 d\Omega_5^2\right)\right]$$

$$\left(\frac{r}{r_H}\right)^2 = \frac{1}{2}\left(\frac{\xi^2}{\xi_H^2} + \frac{\xi_H^2}{\xi^2}\right), \quad f(r) = \left(\frac{1-\xi_H^4/\xi^4}{1+\xi_H^4/\xi^4}\right) \equiv \frac{\omega_-}{\omega_+}, \quad \omega_\pm \equiv 1 \pm \frac{\xi_H^4}{\xi^4}.$$

Holographic WSM with D-instantons

■ Probe D7 brane

- Flavour D7 brane

		x_0	x_1	x_2	x_3	x_4	x_5	x_6	x_7	x_8	x_9
N_C	D3	×	×	×	×						
N_F	D7	×	×	×	×	×	×	×	×		

$$ds_{10}^2 = e^{\Phi/2}\left[\frac{r^2}{L^2}\left(-\frac{\omega_-^2}{\omega_+^2}dt^2 + d\vec{x}^2\right) + \frac{L^2}{\xi^2}\left(d\rho^2 + \rho^2 d\Omega_3^2 + dR^2 + R^2 d\phi^2\right)\right]$$

- WSM: $R = R(\rho), \qquad \phi = bz$
- Induced metric of D7 brane

$$ds_{D7}^2 = e^{\Phi/2}\left[\frac{r^2}{L^2}\left(-\frac{\omega_-^2}{\omega_+^2}dt^2 + \left(dx^2 + dy^2\right)\right) + \left(\frac{r^2}{L^2} + \frac{L^2 b^2 R^2}{\xi^2}\right) dz^2 + \frac{L^2}{\xi^2}\left(\left(1 + R'^2\right) d\rho^2 + \rho^2 d\Omega_3^2\right)\right]$$

Holographic WSM with D-instantons

- Probe D7 brane
  - Flavour D7 brane

		x_0	x_1	x_2	x_3	x_4	x_5	x_6	x_7	x_8	x_9
N_C	D3	×	×	×	×						
N_F	D7	×	×	×	×	×	×	×	×		

$$ds_{10}^2 = e^{\Phi/2}\left[\frac{r^2}{L^2}\left(-\frac{\omega_-^2}{\omega_+^2}dt^2 + d\vec{x}^2\right) + \frac{L^2}{\xi^2}\left(d\rho^2 + \rho^2 d\Omega_3^2 + dR^2 + R^2 d\phi^2\right)\right]$$

  - WSM: $R = R(\rho)$, $\phi = bz$

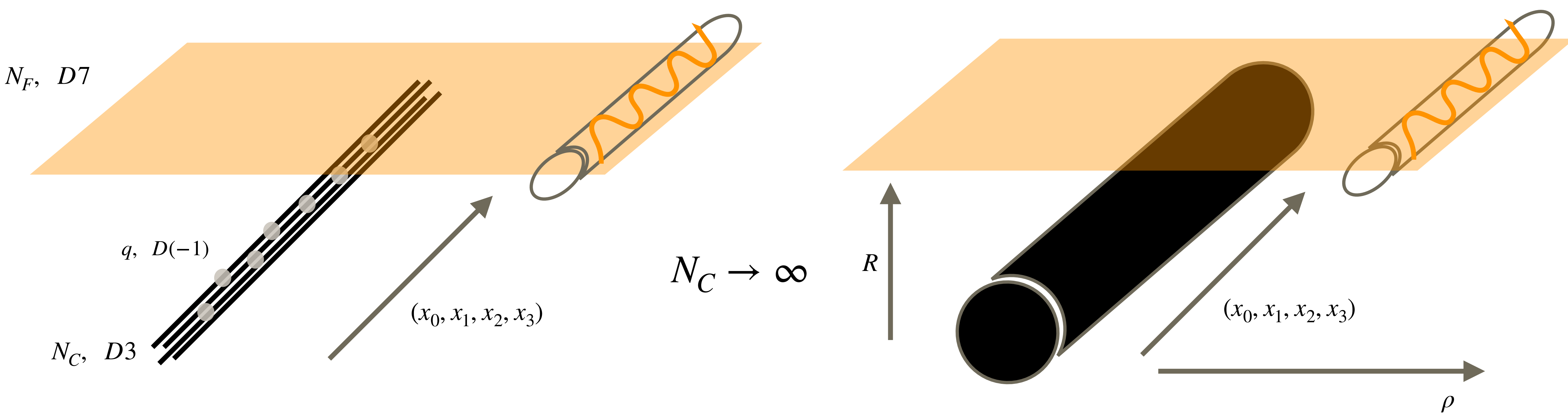

Holographic WSM with D-instantons

- Probe D7 brane
  - DBI action

$$S_{DBI} = -N_F \mu_7 \int d^8\sigma e^{-\Phi} \sqrt{-\det(P[g] + 2\pi\alpha' F)}$$

$$\boxed{\begin{aligned} S_{D7} &\equiv -\tau_7 \int dt d\rho\, V(\rho, R)\sqrt{1+R'^2}, \\ V(\rho, R) &= e^{\Phi}\omega_+\omega_-\rho^3 \sqrt{1+\left(\frac{L^2 bR}{\sqrt{\omega_+}\xi^2}\right)^2}, \quad \tau_7 = 2\pi^2 N_f \mu_7. \end{aligned}}$$

  - Equation of motion

$$\frac{R''}{1+R'^2} + R' \frac{\partial \log V}{\partial \rho} - \frac{\partial \log V}{\partial R} = 0$$

Holographic WSM with D-instantons

- Probe D7 brane
  - b and q effects on the D7 brane embeddings

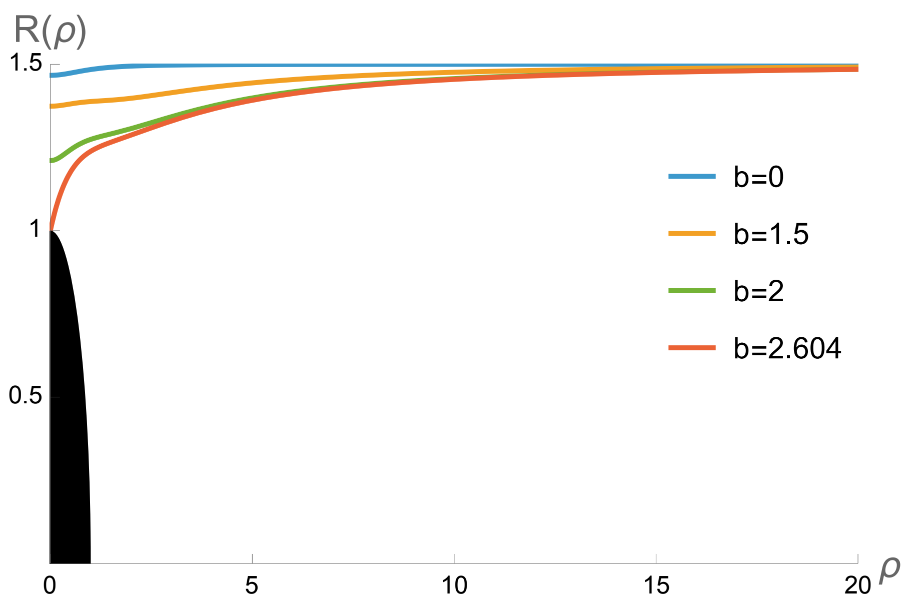

(a) $q = 0,\ m_e = 1.5$

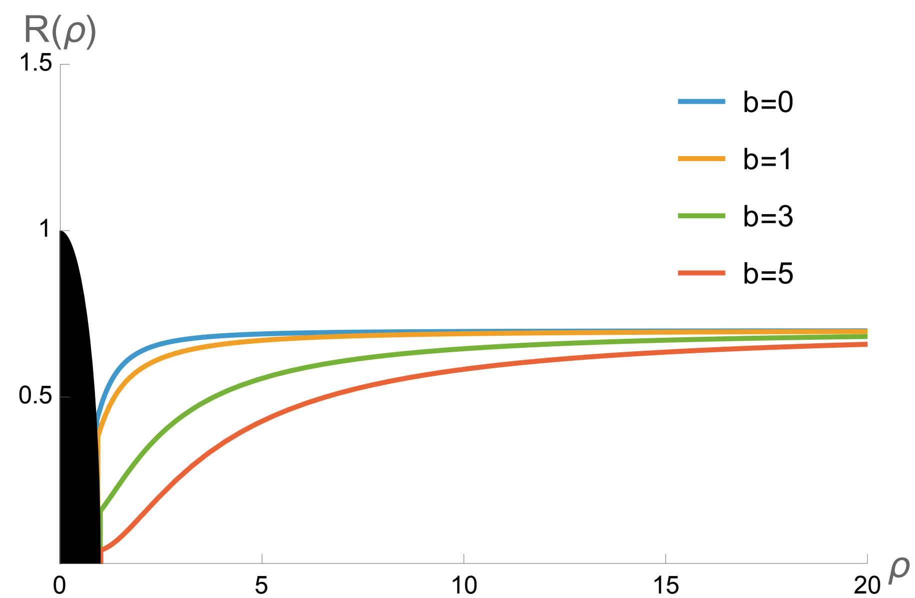

(b) $q = 0,\ m_e = 0.7$

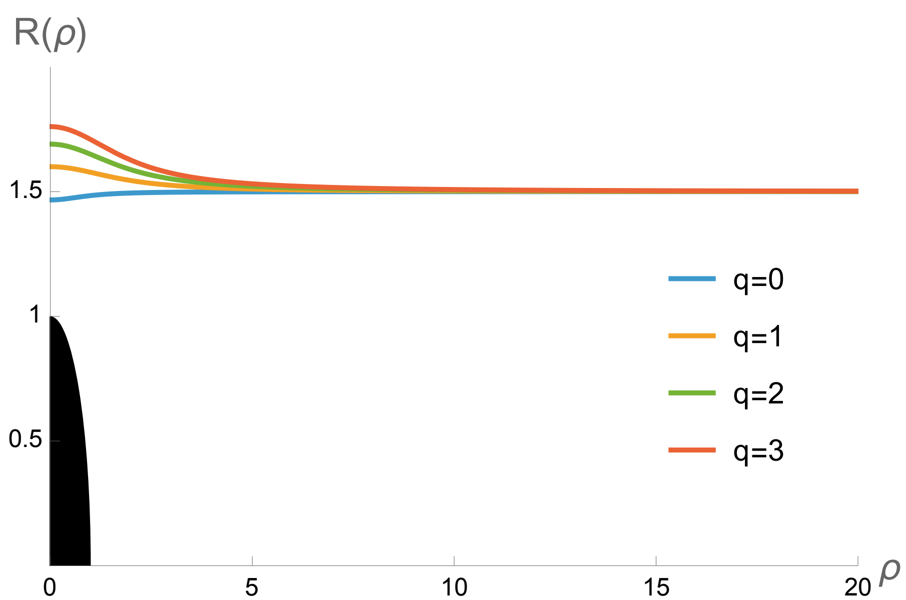

(c) $b = 0,\ m_e = 1.5$

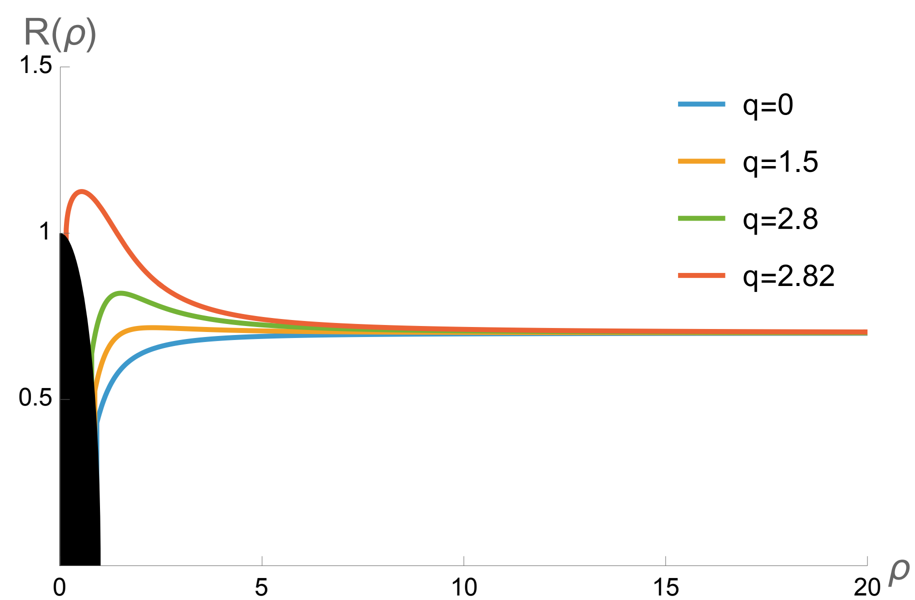

(d) $b = 0,\ m_e = 0.7$

Holographic WSM with D-instantons

- Probe D7 brane
  - Free energy

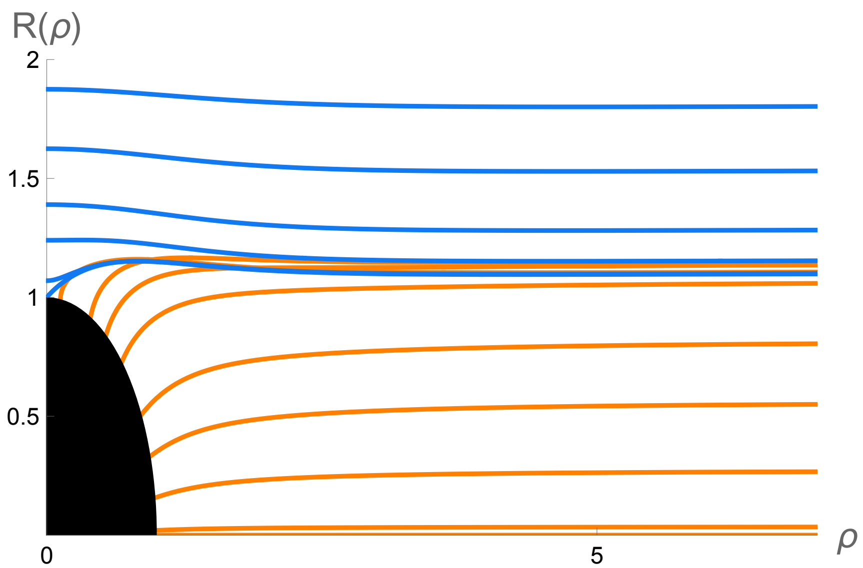

(a) $q/b = 1$

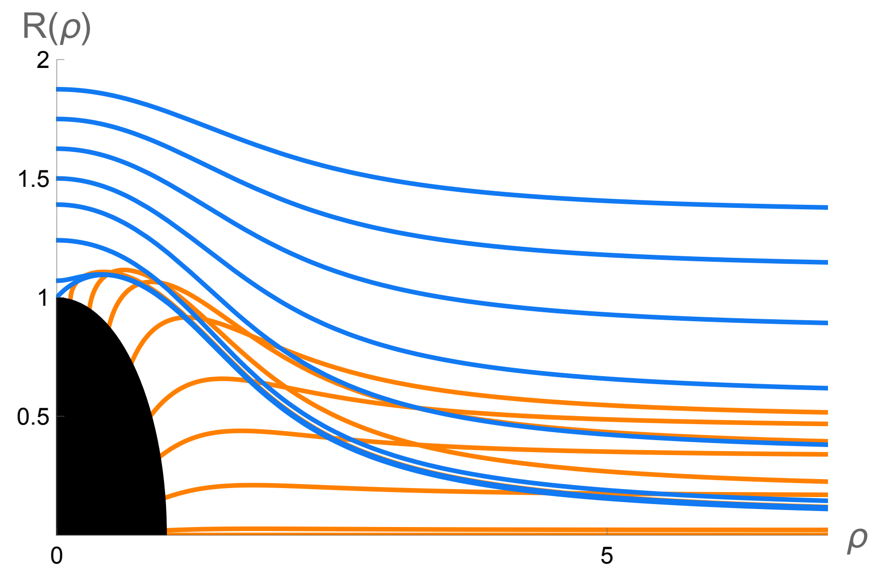

(b) $q/b = 7$

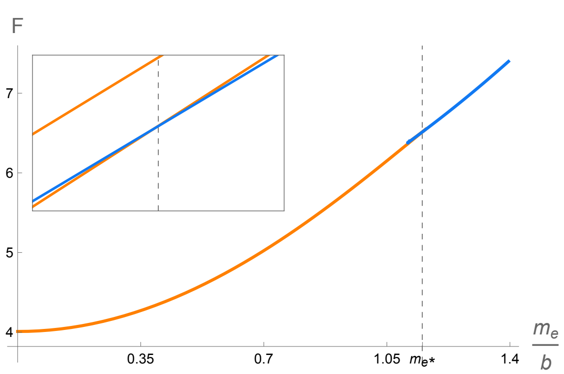

(a) $q/b = 1$

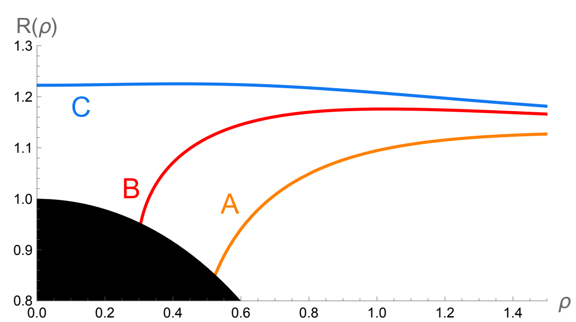

(b) $q/b = 1$

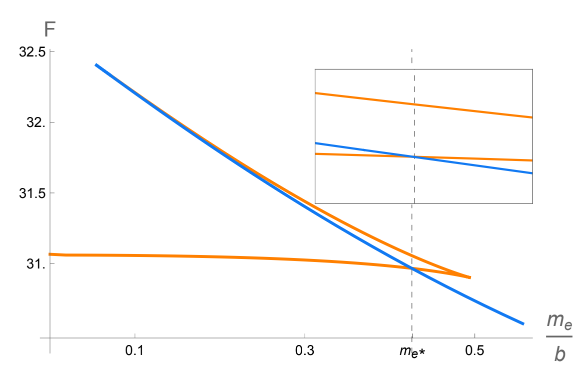

(c) $q/b = 7$

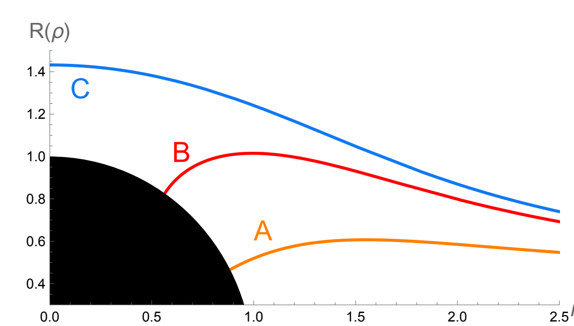

(d) $q/b = 7$

$$F = \tau_7 \left[\int^{\rho_c} d\rho\, V(\rho, R)\sqrt{1 + R'^2} - \frac{1}{4}\rho_c^4 \right]$$

Holographic WSM with D-instantons

■ Phase diagram

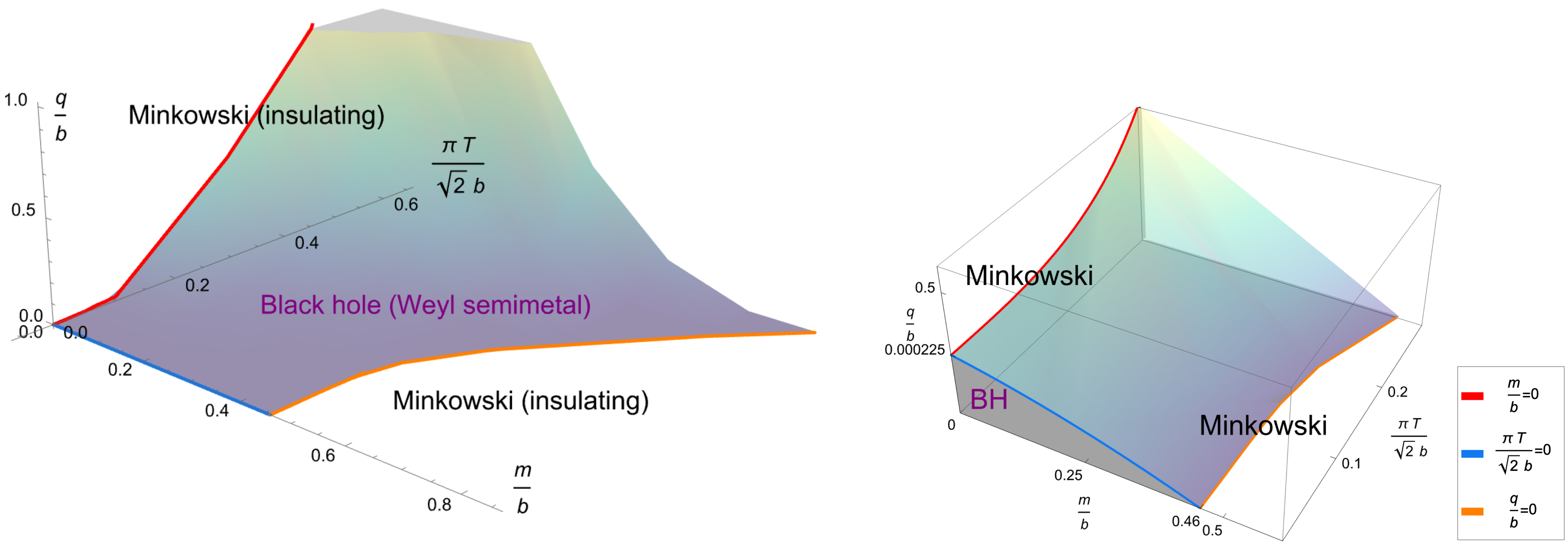

(a) (b)

Holographic WSM with D-instantons

■ Non-linear conductivity

- Fluctuations

$$A_x(t,\rho) = Et + A_x(\rho), \quad A_y(\rho), \quad \phi(z,\rho) = bz + \phi(\rho)$$

- Fluctuation Lagrangian

$$S_{D7} = -\mathcal{N}\int d\rho \left(\sqrt{w_1\left[\omega_+\left(1+R'^2\right)+A_y'^2\right] + w_2\phi'^2 + w_3 A_y'^2} - w_4 Ay'\right),$$

$$w_1(\rho) = \rho^6\left(\frac{L^4 b^4 R^2}{\xi^4}+\omega_+\right)\left(e^\Phi\omega_-^2 - \frac{L^4E^2}{\xi^4}\right), \; w_2(\rho) = \rho^6 e^\Phi R^2\omega_+^2\left(e^\Phi\omega_-^2 - \frac{L^4E^2}{\xi^4}\right)$$
$$w_3(\rho) = \rho^6 e^\Phi\omega_-^2\left(\frac{L^4b^4R^2}{\xi^4}+\omega_+\right), \; w_4(\rho) = \frac{L^4Eb\rho^4}{\xi^4}.$$

- Legendre transformation

$$\begin{aligned}\tilde{S}_{D7} &= S_{D7} - \mathcal{N}\int d\rho\left(\phi' P_\phi + A_x' P_x + A_y' P_y\right)\\ &= -\mathcal{N}\int d\rho\sqrt{\omega_+}\sqrt{1+R'^2}\sqrt{\alpha(\rho)\beta(\rho)-\gamma(\rho)},\end{aligned}$$

$$\alpha(\rho) = e^\Phi\omega_-^2 - \frac{L^4E^2}{\xi^4}, \quad \beta(\rho) = \rho^6\left(\frac{L^4b^4R^2}{\xi^4}+\omega_+\right) - \frac{j_x^2}{e^\Phi\omega_-^2},$$
$$\gamma(\rho) = \left(\frac{L^4b^4R^2}{\xi^4}+\omega_+\right)\frac{p_\phi^2}{\omega_+^2 e^\Phi R^2} + e^\Phi\left(\frac{L^4bE\rho^4}{\xi^4} - j_y\right)^2.$$

$$P_\phi = \mathcal{N}p_\phi, \; P_x = \mathcal{N}j_x, \; P_y = \mathcal{N}j_y$$

Holographic WSM with D-instantons

■ Non-linear conductivity

- Fluctuation Hamiltonian should be regular at the world volume horizon($\rho = \rho_*$)

$$\alpha(\rho_*) = 0, \quad \beta(\rho_*) = 0, \quad \gamma(\rho_*) = 0$$

$$\alpha(\rho) = e^{\Phi}\omega_-^2 - \frac{L^4E^2}{\xi^4}, \quad \beta(\rho) = \rho^6\left(\frac{L^4b^4R^2}{\xi^4} + \omega_+\right) - \frac{j_x^2}{e^{\Phi}\omega_-^2},$$
$$\gamma(\rho) = \left(\frac{L^4b^4R^2}{\xi^4} + \omega_+\right)\frac{p_\phi^2}{\omega_+^2 e^{\Phi}R^2} + e^{\Phi}\left(\frac{L^4bE\rho^4}{\xi^4} - j_y\right)^2.$$

- Currents
  - Black hole embedding

$$\langle J_x\rangle = (2\pi\alpha')\mathcal{N}\frac{L^2\rho_*^3E}{\xi_*^2}\sqrt{\frac{L^4b^4R_*^2}{\xi_*^4} + \omega_{+*}}, \quad \langle J_y\rangle = -(2\pi\alpha')\mathcal{N}\frac{L^4bE\rho_*^4}{\xi_*^4}.$$

  - Minkowski embedding

$$\langle J_x\rangle = 0, \quad \langle J_y\rangle = 0$$

Holographic WSM with D-instantons

■ Non-linear conductivity

- Currents
  - Black hole embedding

$$\langle J_x \rangle = (2\pi\alpha')\mathcal{N}\frac{L^2\rho_*^3 E}{\xi_*^2}\sqrt{\frac{L^4 b^4 R_*^2}{\xi_*^4}+\omega_{+*}}, \quad \langle J_y \rangle = -(2\pi\alpha')\mathcal{N}\frac{L^4 b E\rho_*^4}{\xi_*^4}.$$

  - Minkowski embedding

$$\langle J_x \rangle = 0, \quad \langle J_y \rangle = 0$$

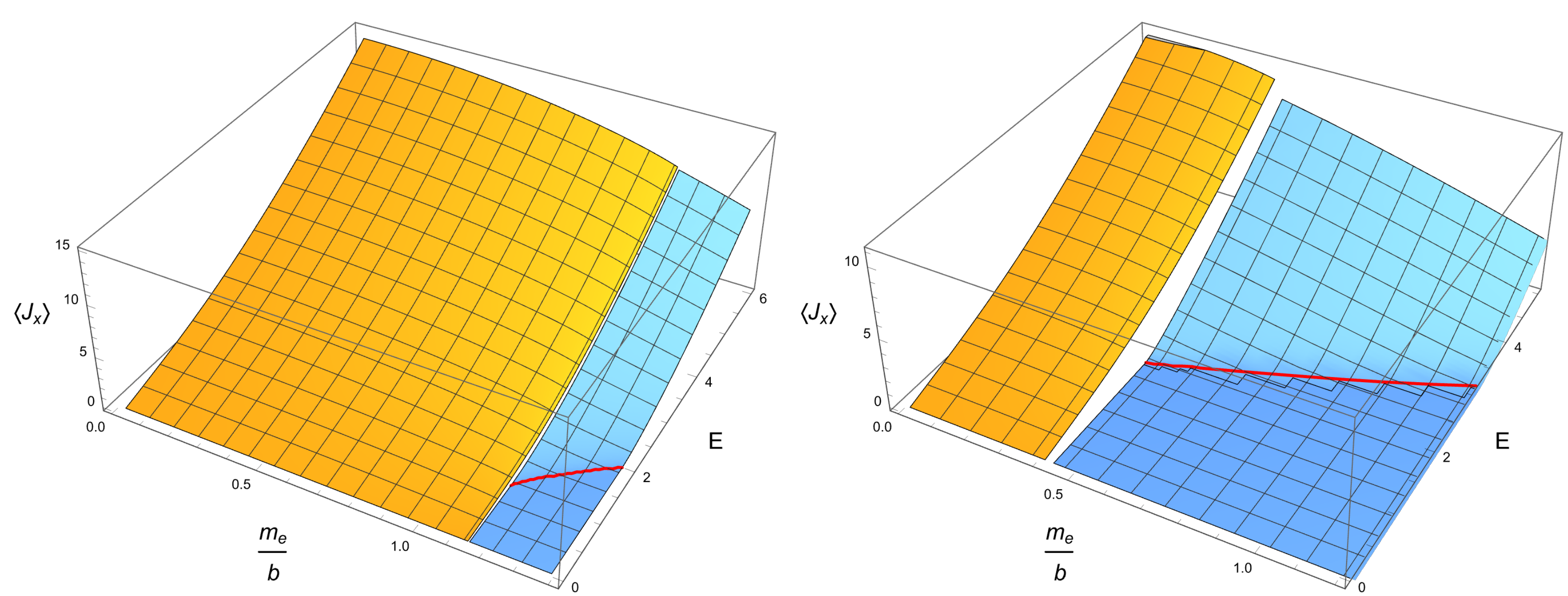

(a) $q = 1$ (b) $q = 7$

Holographic WSM with D-instantons

Non-linear conductivity

- Currents
  - Black hole embedding

$$\langle J_x\rangle = (2\pi\alpha')\mathcal{N}\frac{L^2\rho_*^3 E}{\xi_*^2}\sqrt{\frac{L^4 b^4 R_*^2}{\xi_*^4}+\omega_{+*}},\quad \langle J_y\rangle = -(2\pi\alpha')\mathcal{N}\frac{L^4 b E\rho_*^4}{\xi_*^4}.$$

  - Minkowski embedding

$$\langle J_x\rangle = 0,\quad \langle J_y\rangle = 0$$

- DC conductivities

$$\sigma_{xx} = \lim_{E\to 0}(2\pi\alpha')\langle J_x\rangle/E,\qquad \sigma_{xy} = -\sigma_{yx} = -\lim_{E\to 0}(2\pi\alpha')\langle J_y\rangle/E$$

$$\sigma_{xx} = \lim_{E\to 0}(2\pi\alpha')^2\mathcal{N}\frac{L^2\rho_H^3}{\xi_H^2}\sqrt{\frac{L^4 b^4 R_H^2}{\xi_H^4}+\omega_{+H}},\quad \sigma_{xy} = -\lim_{E\to 0}(2\pi\alpha')^2\mathcal{N}\frac{L^4 b\rho_H^4}{\xi_H^4}.$$

Holographic WSM with D-instantons

■ DC conductivities

- WSM to insulator transition

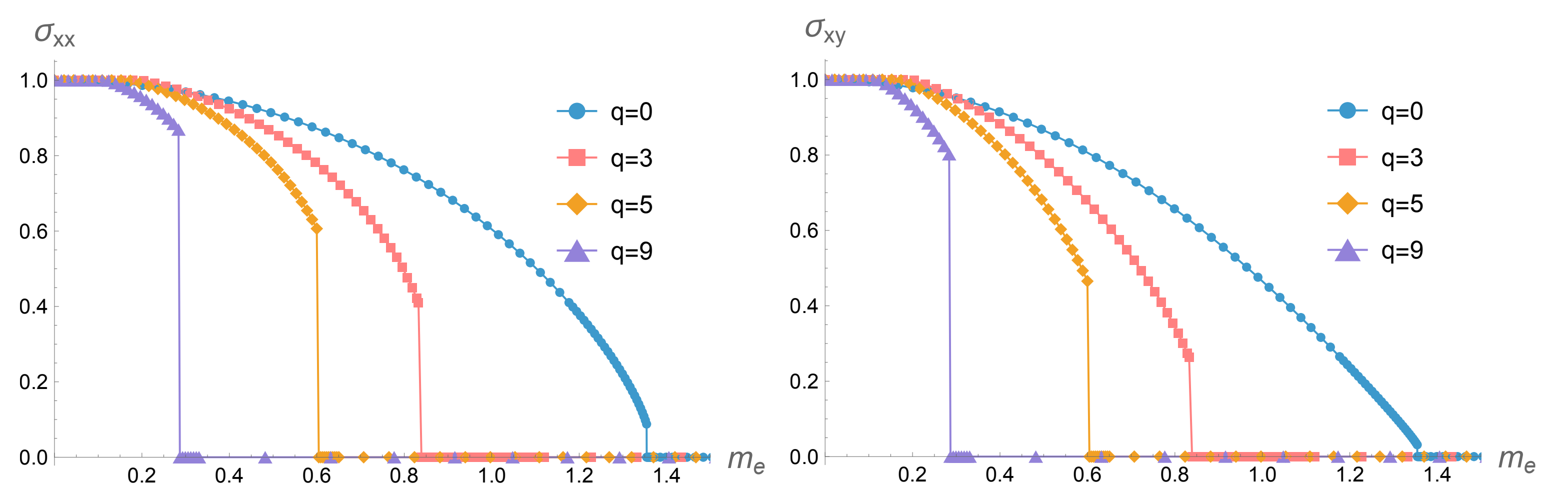

(a) Longitudinal conductivity σ_{xx} (b) Hall conductivity σ_{xy}

Figure 5: Conductivities for $\xi_H = 1$ and $b = 1$. $(T/b \approx 0.45)$

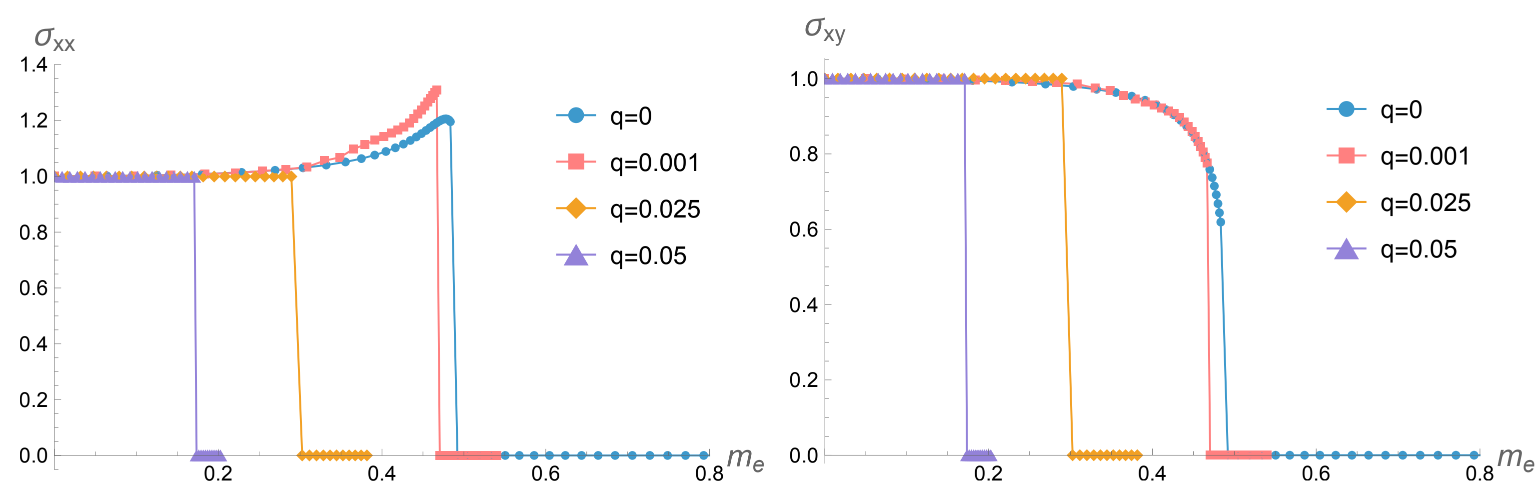

(a) Longitudinal conductivity σ_{xx} (b) Hall conductivity σ_{xy}

Figure 6: Conductivities for $\xi_H = 0.2$ and $b = 1$. $(T/b \approx 0.09)$

Holographic WSM with D-instantons

- DC conductivities
  - WSM to insulator transition

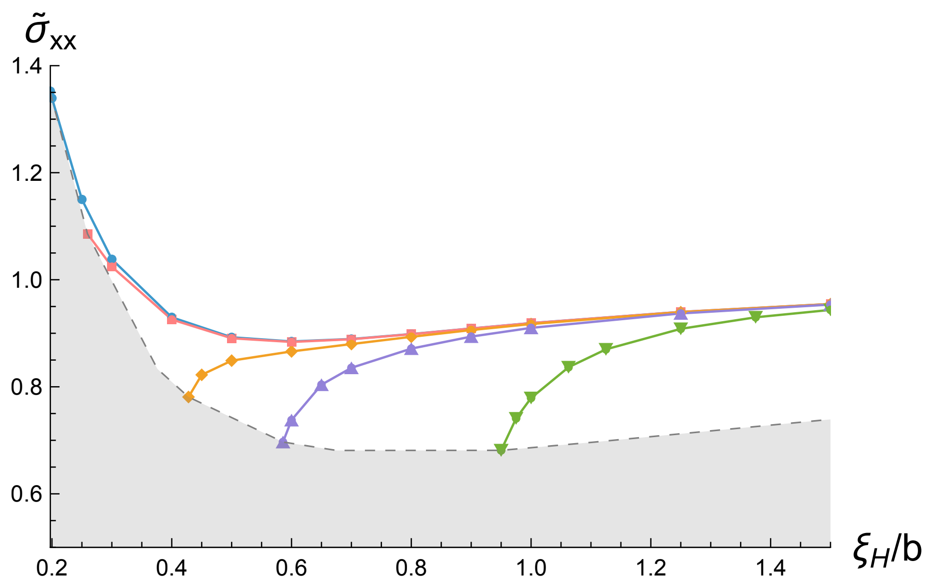

(a) Longitudinal conductivity σ_{xx}

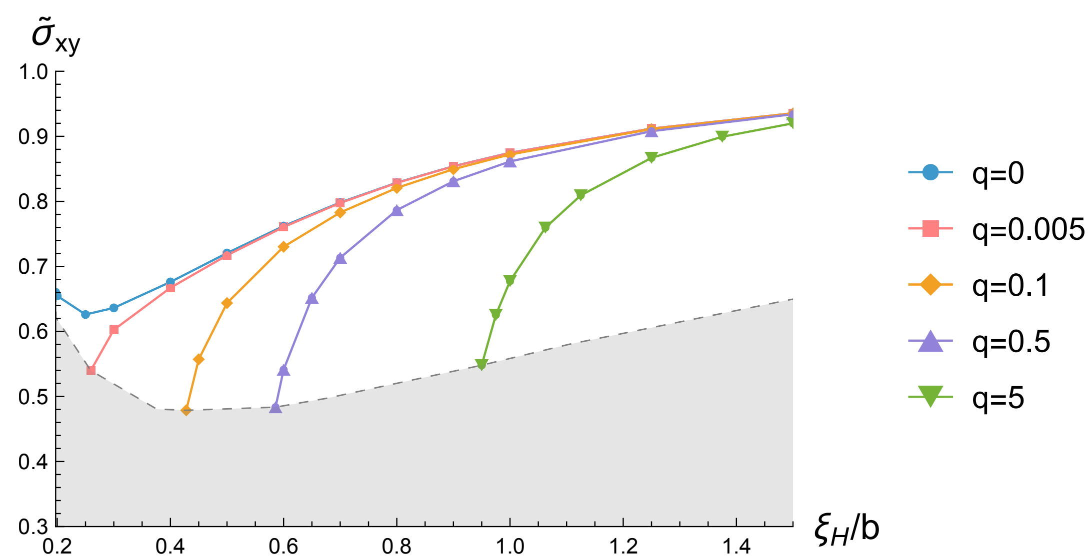

(b) Hall conductivity σ_{xy}

Holographic WSM with D-instantons

■ Gap Oppening Process

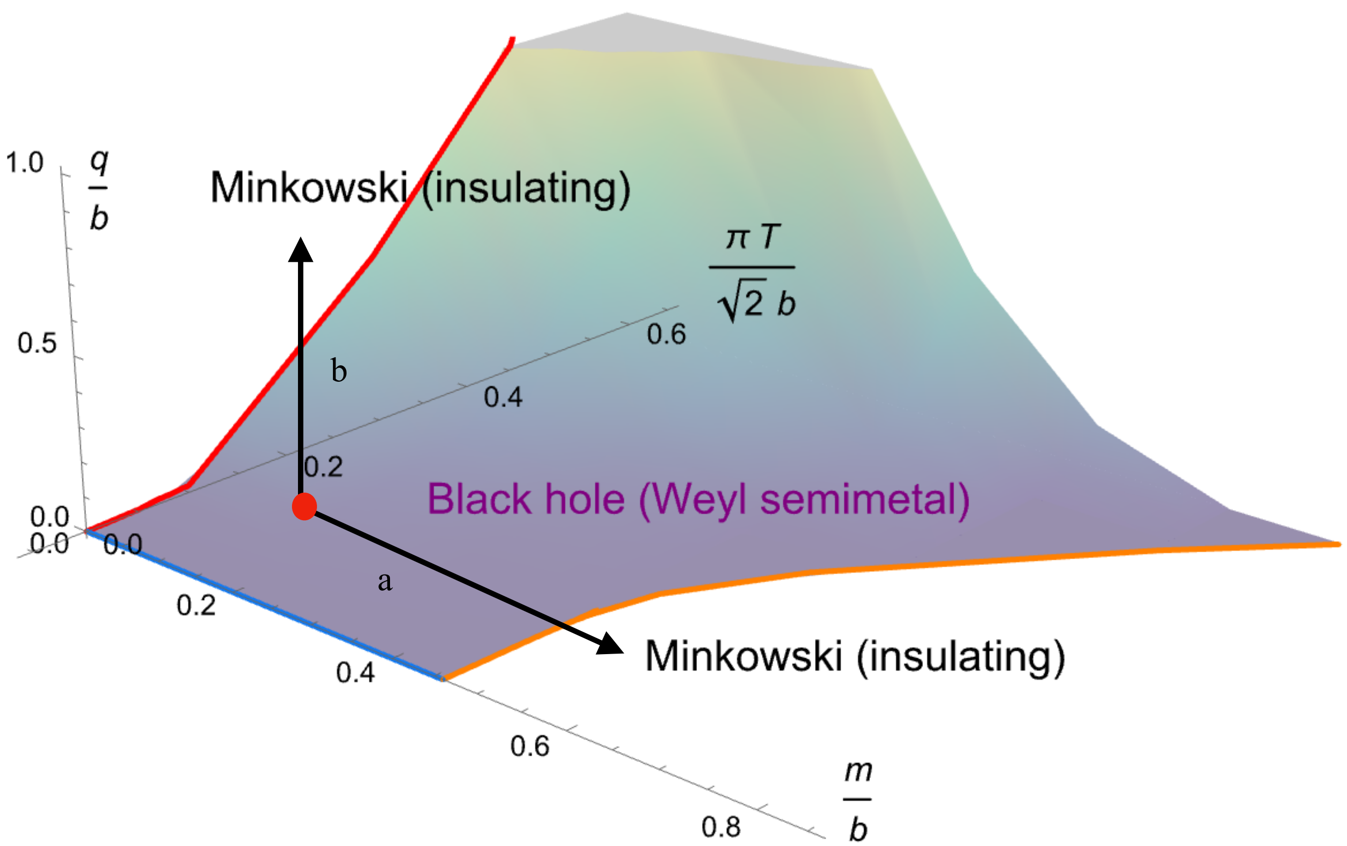

Holographic WSM with D-instantons

■ Gap Oppening Process

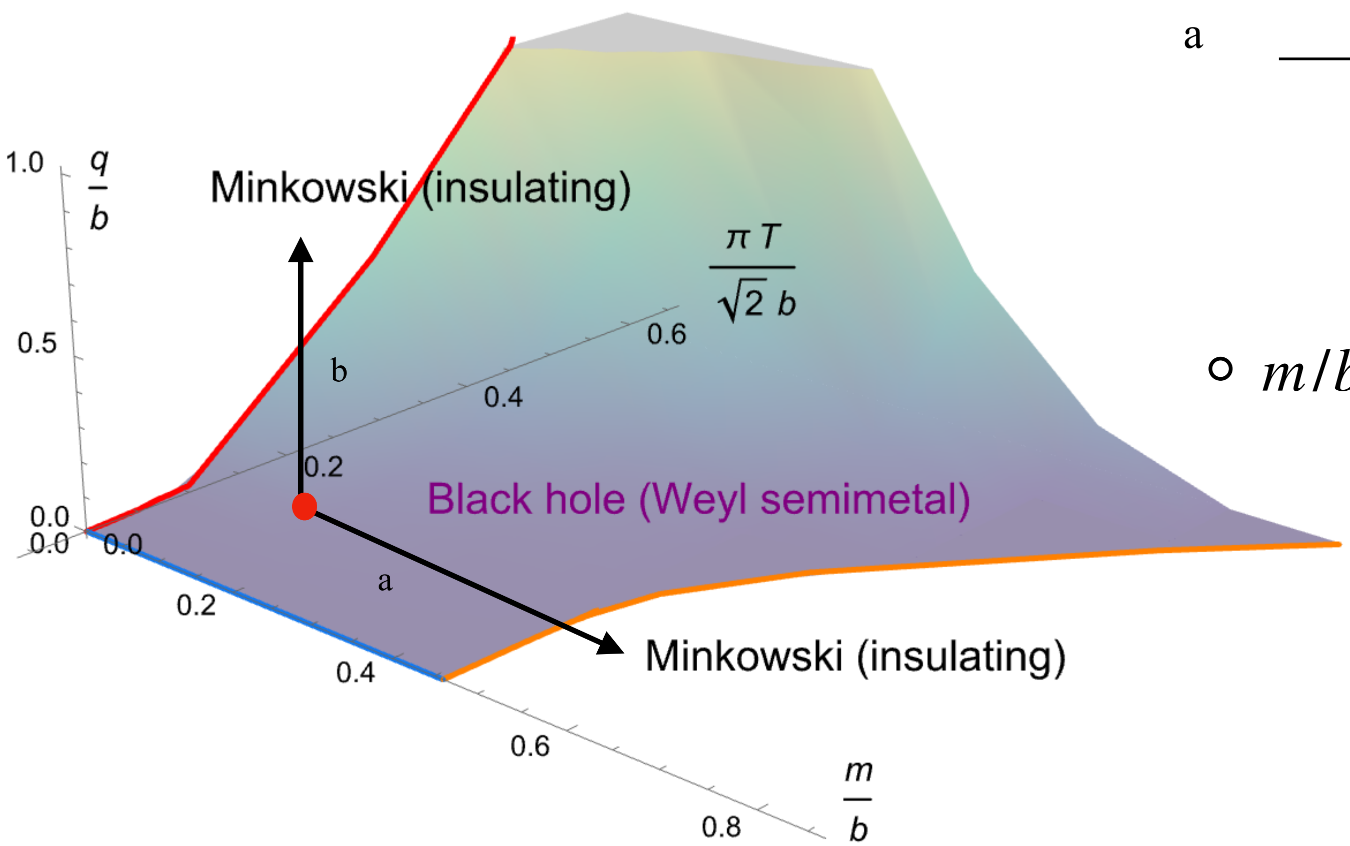

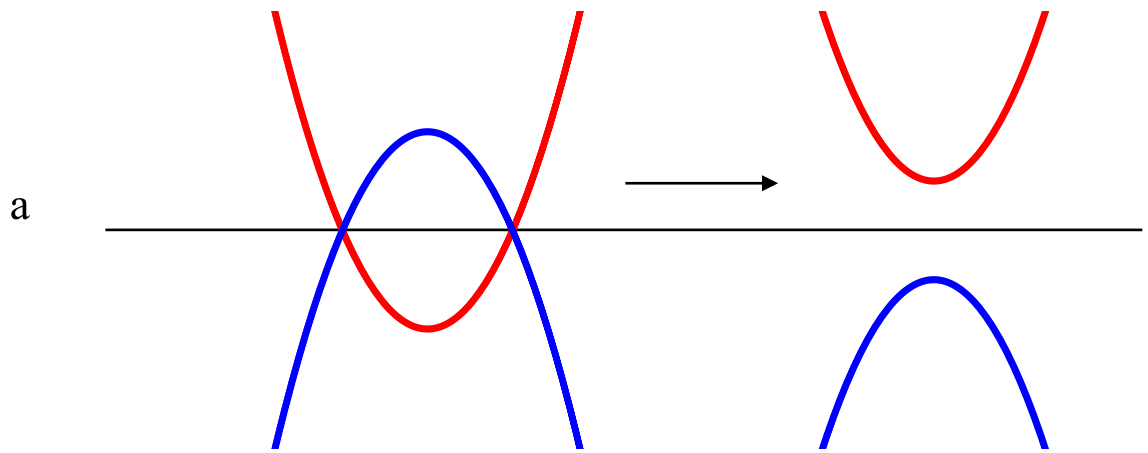

○ m/b-induced: explicit chiral symmetry breaking

Holographic WSM with D-instantons

■ Gap Oppening Process

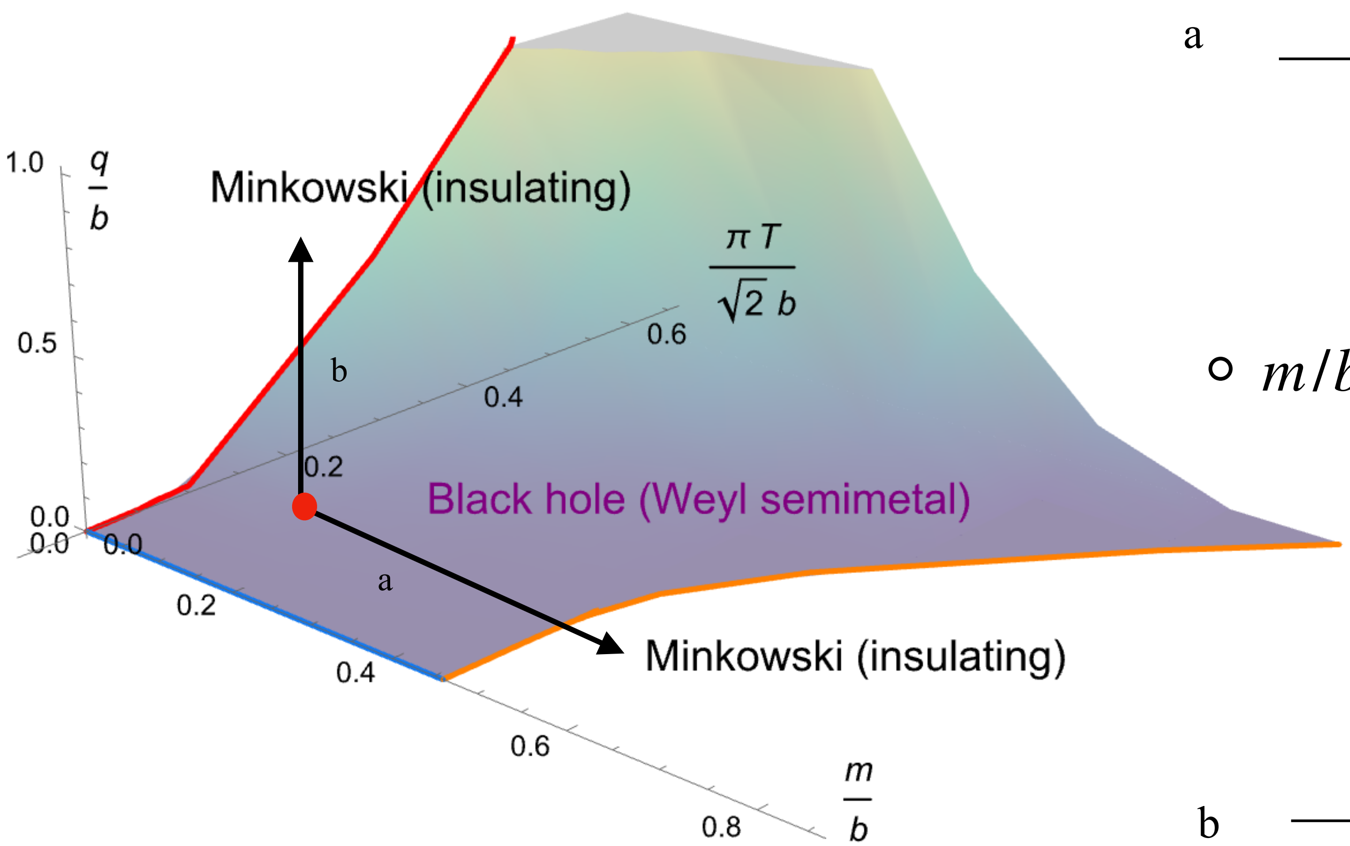

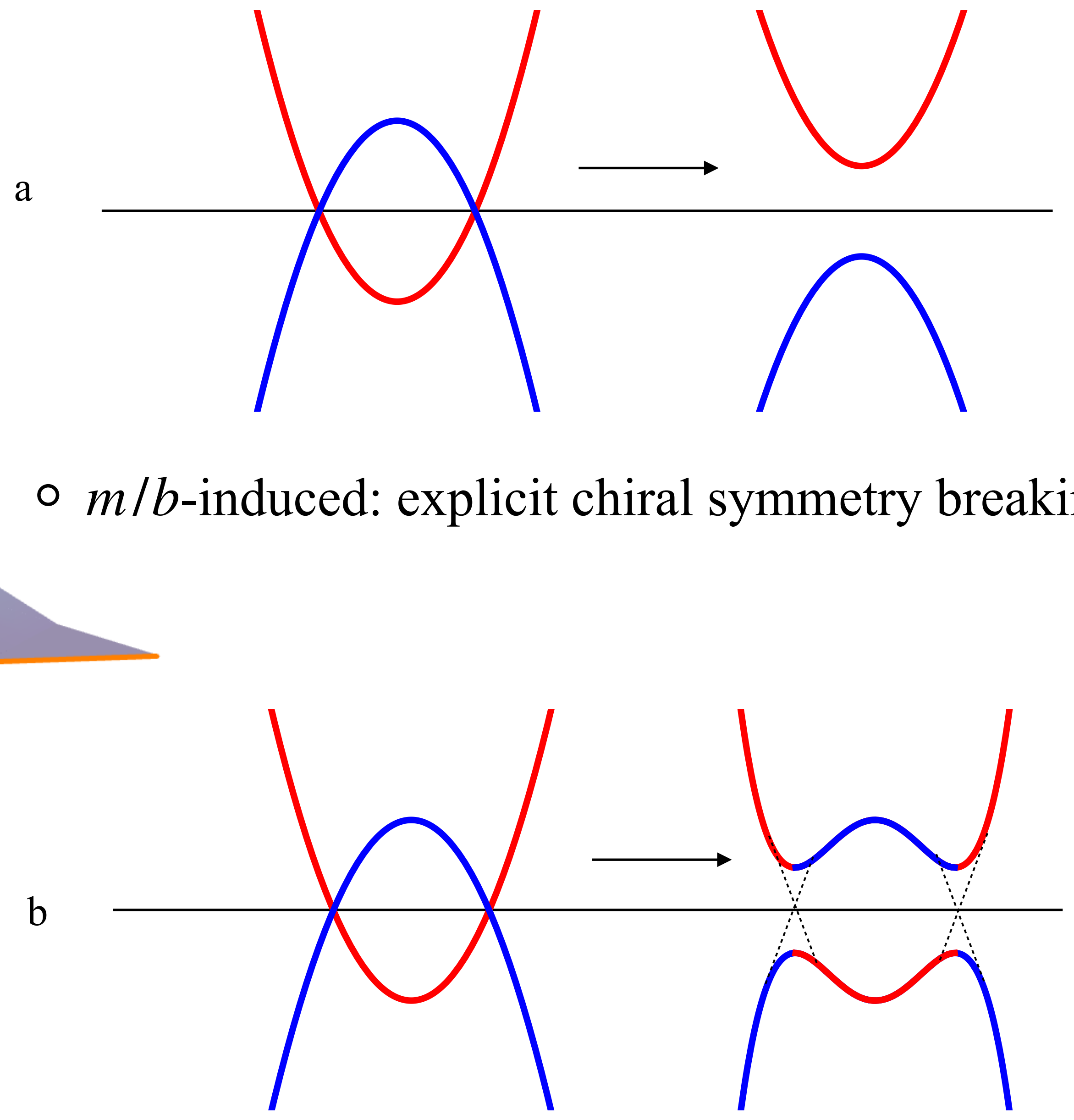

- m/b-induced: explicit chiral symmetry breaking
- q/b-induced: spontaneous chiral symmetry breaking

Conclusion and Discussion

- We study D-instanton effects on the holographic Weyl semimetal
- For given Weyl point and electron mass, instanton impurities can make WSM-insulator trantision
- What is a interpretation of the D-instanton impurities in condensed matter physics?
- WSM-TI transtion? We need to introduce boundaries

Thank you !!